Redox Biology 12 (2017) 987–1003

Contents lists available at ScienceDirect

Redox Biology

journal homepage: www.elsevier.com/locate/redox

Research Paper

The role of sodium hydrosulfide in attenuating the aging process *via* PI3K/AKT and CaMKKβ/AMPK pathways

Xubo Chen[a,1], Xueyan Zhao[a,1], Hua Cai[a], Haiying Sun[a], Yujuan Hu[a], Xiang Huang[a], Wen Kong[b,*], Weijia Kong[a,*]

[a] Department of Otorhinolaryngology, Union Hospital of Tongji Medical College, Huazhong University of Science and Technology, Wuhan 430022, China
[b] Department of Endocrinology, Union Hospital of Tongji Medical College, Huazhong University of Science and Technology, Wuhan 430022, China

ARTICLE INFO

Keywords:
Aging
Hydrogen sulfide
ROS
Mitochondria
PI3K/AKT
CaMKKβ/AMPK

ABSTRACT

Age-related dysfunction of the central auditory system, known as central presbycusis, is characterized by defects in speech perception and sound localization. It is important to determine the pathogenesis of central presbycusis in order to explore a feasible and effective intervention method. Recent work has provided fascinating insight into the beneficial function of H_2S on oxidative stress and stress-related disease. In this study, we investigated the pathogenesis of central presbycusis and tried to explore the mechanism of H_2S action on different aspects of aging by utilizing a mimetic aging rat and senescent cellular model. Our results indicate that NaHS decreased oxidative stress and apoptosis levels in an aging model *via* CaMKKβ and PI3K/AKT signaling pathways. Moreover, we found that NaHS restored the decreased activity of antioxidants such as GSH, SOD and CAT in the aging model *in vivo* and *in vitro* by regulating CaMKKβ and PI3K/AKT. Mitochondria function was preserved by NaHS, as indicated by the following: DNA POLG and OGG-1, the base excision repair enzymes in mitochondrial, were upregulated; OXPHOS activity was downregulated; mitochondrial membrane potential was restored; ATP production was increased; and mtDNA damage, indicated by the common deletion (CD), declined. These effects were also achieved by activating CaMKKβ/AMPK and PI3K/AKT signaling pathways. Lastly, protein homeostasis, indicated by HSP90 alpha, was strengthened by NaHS *via* CaMKKβ and PI3K/AKT. Our findings demonstrate that the ability to resist oxidative stress and mitochondria function are both decreased as aging developed; however, NaHS, a novel free radical scavenger and mitochondrial protective agent, precludes the process of oxidative damage by activating CaMKKβ and PI3K/AKT. This study might provide a therapeutic target for aging and age-related disease.

1. Introduction

In addition to genetic factors, oxidative stress is a major contributor to age-related disorders such as cognitive decline, senile dementia and presbycusis (also called age-related hearing loss). Accumulation of damage caused by oxidative stress is recognized as accountable for the development of aging and is tightly related with mitochondria dysfunction [1]. Reactive oxygen species (ROS) is an inevitable byproduct during the process of oxidative phosphorylation in aerobic metabolism and originates in the electron transport chain of mitochondria. An imbalance between the generation and ablation of ROS causes the occurrence of oxidative stress and results in oxidative damage [2]. Mitochondria not only play an important role in initiating aging though the production of ROS but also become a susceptible target of oxidative stress. For example, unlike nuclear DNA, mitochondrial DNA (mtDNA) is not coated with histone proteins; therefore, they are sensitive to oxidative stress and any deletions and/or mutations accumulate during the aging process [3], including the 4834-base-pair (bp) deletion in rats and 4977-bp deletion in humans, which are known as the common deletion (CD) and act as an accurate biomarker [4–6] of aging. The mtDNA is essential for mitochondrial function, even though it encodes only 13 mitochondrial proteins [7]. Thus, as aging proceeds and

Abbreviations: D-gal, D-galactose; H_2S, Hydrogen Sulfide; ROS, Reactive Oxygen Species; CD, Common Deletion; GSH, Glutathione; SOD, Superoxide Dismutase; DMEM, Dulbecco's Modified Eagle Medium; PI3K, Phosphatidylinositol 3-kinase; CaMKKβ, Ca2+/calmodulin-dependent protein kinase kinase β; AMPK, AMP-activated Protein Kinase; PRDX2 or Prx-2, Peroxiredoxin 2; TXNRD1, Thioredoxin Reductase 1; DNA POLG, DNA Polymerase Gamma; OGG1, 8-oxoG DNA glycosylase 1; HSP90, Heat Shock Protein 90; NaHS, Sodium Hydrosulfide; OXPHOS, Oxidative Phosphorylation; ATP, Adenosine Triphosphate; GFAP, Glial Fibrillary Acidic Protein; ΔΨm, Mitochondrial Membrane Potential; ANOVA, Analysis of Variance

* Corresponding authors.
E-mail addresses: wenly-kong@163.com (W. Kong), entwjkong@hust.edu.cn (W. Kong).
[1] These authors contributed equally to this work.

http://dx.doi.org/10.1016/j.redox.2017.04.031
Received 28 March 2017; Received in revised form 16 April 2017; Accepted 23 April 2017
Available online 25 April 2017

mtDNA deletions and/or mutations increase, mitochondrial function decreases [8] and oxidative stress is hastened due to the increased production of ROS. As a result, a “vicious cycle” forms, and the aging process accelerates. Furthermore, the function of antioxidants also declines during aging. The antioxidant system includes a number of antioxidant enzymes such as catalase (CAT) and superoxide dismutase (SOD), nonenzymatic antioxidants such as glutathione (GSH) and dietary antioxidants. As reported previously, aged rats suffered from decreased antioxidant capacity, as compared with young rats [9]. As antioxidants play a crucial role against ROS, an impaired antioxidant system aggravates the process of aging and may become another “vicious cycle”. In addition to oxidation, surveillance of the proteome and the ability to maintain protein homeostasis also declines during aging [10], facilitating the emergence of age-related degenerative diseases caused by protein aggregation such as Alzheimer's disease and Parkinson's disease. Therefore, abnormal protein structures caused by dysfunctional protein homeostasis may also promote the process of aging. As stated above, aging is complex, with interactions among several pathophysiological processes. Though many studies focused on the pathogenesis of aging and oxidative stress, effective intervention measures are still being explored. Some studies demonstrated that drugs utilizing antioxidation showed attenuation to some extent. In clinics, vitamin E supplementation and anti-neuroinflammatory drugs are two major therapeutic approaches that are used to treat neurodegenerative diseases [11]. Exogenous antioxidants, such as rutin and sulfur compounds, are commonly utilized approaches in experimental studies to intervene in aging by activating survival pathways such as phosphatidylinositol 3-kinase/protein kinase B (PI3K/AKT) and inhibiting the occurrence of apoptosis [12,13]. However, to our knowledge, little literature is available concerning whether and how these antioxidants regulated the upstream factors of apoptosis, such as protein homeostasis, mtDNA repair enzymes and the endogenous antioxidants.

Hydrogen sulfide (H_2S) is one of the three important gastrotransmitters (H_2S, NO, CO), it has a double-side effect [14]: when in a very high level, it is poisonous while in a low level, it plays a beneficial effects. H_2S is an endogenously synthesized and regulates a wide range of pathophysiological processes involving autophagy, cell metabolism, inflammation, cell cycle and oxidative stress [15]. According to some studies, reduced H_2S is closely related to the development of aging. It was found that the plasma H_2S level declined in an age-dependent manner in human subjects who were 50–80 years old [16]; furthermore, H_2S was reported to ameliorate insulin resistance and improve glucose uptake in type 2 diabetic models [17], which suggested a positive effect of H_2S on inhibiting the pathogenesis of aging and age-related diseases. In addition, some studies reported that exogenous H_2S contributed to the defense against oxidative damage [18,19] and inhibition of apoptosis and the autophagy pathway [20], which are also related to regulating the aging process [21]. The PI3K/AKT pathway is commonly recognized as a key signaling pathway controlling autophagy [22] and metabolism [23], as well as oxidative stress. Thus, the PI3K/AKT signaling pathway could be a therapeutic target under some oxidative stress conditions, such as the process of aging. AMP-activated protein kinase (AMPK)-regulated pathways that direct various metabolic processes have also been explored by many researchers in recent years. As reported, AMPK plays a role in growth arrest and autophagy as a potential survival pathway for cancer cells, while inhibition of AMPK led to the death of cancer cells by autophagy [24]. Furthermore, AMPK also regulates longevity in a number of species, which is attributed to the crucial role of AMPK in metabolic remodeling through many different pathways [25]. Therefore, the AMPK pathway should be another potential therapeutic target for aging and age-related diseases. Despite the reports that H_2S plays a beneficial role in the prevention of oxidative damage and apoptosis [17,20], whether and how H_2S counteracts aging and aging-related accelerators such as mtDNA mutations and repair, mitochondrial dysfunction, disturbed protein homeostasis and imbalanced ROS production is rarely reported. Likewise, whether PI3K/AKT and AMPK signaling pathways are involved in the prevention of the aging process is unclear.

Presbycusis is a disease of age-related degeneration of the auditory system. At present, it is generally accepted that there are at least two components of presbycusis, as follows: a peripheral component involving cochlear degeneration and a central component involving degeneration of the auditory cortex in the central nervous system [26]. D-galactose (D-gal) is widely used in experimental studies to establish mimetic aging model [5,27,28]. After treated with D-gal, pathology of central presbycusis demonstrated increased neural apoptosis and neural damage as well as a decreased number of neurons in the auditory cortex and exhibited degraded cognitive function, which is similar with the natural aging process [27,29,30]. Additionally, our previous study also replicate the central presbycusis with D-gal and causes accumulation of the CD that was also observed in the natural aging animals [29,31]. In our study, we explored the *in vitro* and *in vivo* mechanism for whether and how H_2S acts on contributors of aging in the auditory cortex using a mimetic aging model induced by D-gal. Briefly, we studied how H_2S improves the antioxidant capacity, such as through the activity of SOD, GSH and CAT and the expression level of molecular chaperons. We also examined how H_2S protects mitochondria function, such as *via* the effects on mitochondrial membrane potential ($\Delta\Psi m$), the occurrence of the CD of mtDNA and the repair capability of mtDNA. Furthermore, we also tried to explore the relationship between the molecular changes mentioned above and the signaling pathways of PI3K/AKT as well as AMPK and its upstream kinase, calcium/calmodulin-dependent protein kinase kinase 2 (CaMKK2, also named CaMKKβ). The present study may provide new insight for the application of H_2S in the medical intervention of the aging process and provide a theoretical reference for health promotion.

2. Materials and methods

2.1. Animals

Male 3-week-old Sprague-Dawley (SD) rats, with an initial weight of 80–100 g, were purchased from the experimental animal center of Tongji Medical College, Huazhong University of Science and Technology (HUST). The animals were acclimated in conditions of 50% humidity and 25 °C room temperature, with a quiet environment and 12 h/12 h light/dark cycle. Standard rodent chow and water were adequately provided. Each animal was marked with trinitrophenol, followed by random separation into two groups. (1) The first group was subcutaneously injected with D-gal (dissolved in normal saline, 500 mg/kg/day for 8 weeks; Sigma Aldrich Corp., St Louis, MO, USA) for the mimetic aging model. After the schedule was finished (3 months of age), the 3-month-old mimetic aging rats were treated as follows: one subgroup was injected intraperitoneally with NaHS (dissolved in normal saline, 1.4 mg/kg/day) for 10 days before sacrifice (**3-month-old mimetic aging + NaHS group**); another subgroup was injected with normal saline intraperitoneally for 10 days as a comparison (**3-month-old mimetic aging group**); a third subgroup was kept on normal chow for six months and then divided into 2 subgroups, with one subgroup injected with NaHS (1.4 mg/kg/day) for 10 days intraperitoneally before sacrifice (**9-month-old mimetic aging + NaHS group**) and the other subgroup injected with normal saline intraperitoneally for 10 days as a comparison (**9-month-old mimetic aging group**). (2) To control for D-gal, the second group was injected with normal saline subcutaneously on the same schedule, followed by separation into 2 subgroups, with one subgroup injected with normal saline intraperitoneally for 10 days as a control (**3-month-old control group**) and the other subgroup kept on normal feeding for 6 months and then injected with normal saline intraperitoneally for 10 days as a counterpart (**9-month-old control group**). Treatment of each subgroup of the rats is also described in Supplementary information Fig.

S1a. All the experimental procedures were in accordance with the National Institutes of Health "Guide for the Care and Use of Laboratory Animals" (NIH Publications No. 80-23, revised 1996) and approved by the Committee on Animal Research of Tongji Medical College, HUST.

2.2. Primary culture of auditory cortex neurons

The culture procedure of auditory cortex neurons was published previously [32], with a few modifications. Briefly, brains were dissected from neonatal rats (< 48 h) in cold D-Hanks solution, and the auditory cortex was dissociated from the brains in Dulbecco's modified Eagle's medium (DMEM; Hyclone, Logan, UT, USA). Cells were obtained by digestion in 1.25% trypsin at 37 °C for 10 min followed by mild mechanical dissociation in DMEM. Cultures were grown on polylysine-coated coverslips or plates in DMEM supplemented with 10% (v/v) fetal bovine serum (FBS, Gibco, Grand Island, NY, USA). Six hours later and after the cells were attached, the medium was then changed to serum-free 10% B-27-supplemented neurobasal medium (Gibco, Grand Island, NY, USA). About 30–50% of the medium was changed every 3 days. After 7 days, the neurons were treated with D-gal, which was dissolved in serum-free 10% B-27- supplemented neurobasal medium, for another 7 days, with 30–50% of the medium also changed every 3 days during this period. Chemical inhibitors were incubated with the D-gal pretreated neurons for 40 mins, and the neurons were incubated with NaHS for another 24 h. All the neurons were cultured at 37 °C in a 5% CO_2 incubator. Treatment of each subgroup of the neurons is also described in Supplementary information Fig. S1b.

2.3. Cell viability and cell senescent tests

Cells were cultured on a 48-well plate and treated with increasing concentrations of D-gal for 7 days. Cell viability was then measured by the cell counting kit-8 (CCK-8) (Dojindo Laboratories, Kumamoto, Japan) according to the manufacturer's instructions. Cell senescent was evaluated by a Senescence β-Galactosidase Staining Kit (C0602, Beyotime, Haimen, China) according to the manufacturer's instructions.

2.4. Immunohistochemistry (IHC) analysis

Rats used for immunohistochemistry analysis were transcardially perfused with about 400 ml of saline followed by 4% paraformaldehyde solution (pH = 7.2–7.4). The brains were removed and postfixed in 4% paraformaldehyde overnight at 4 °C. The selection and orientation of the auditory cortex and the following procedures were previously published [33]. Primary antibodies against cleaved-caspase-3 (1:500, servicebio, Wuhan, Hubei, China) and glial fibrillary acidic protein (GFAP; 1:1000, Proteintech, Wuhan, Hubei, China) were used for the IHC analysis. After being mounted with neutral balsam, the sections were observed by standard microscopy (DM2500, Leica Microsystems Wetzlar GmbH, Wetzlar, Germany).

2.5. Measurement of oxidants and antioxidant enzyme activities

The levels of total-SOD (A001-1, Nanjing, Jiangsu, China) and GSH (A006-1, Nanjing, Jiangsu, China) were measured in the plasma of the rats and in the cultured neurons. The level of CAT (A007-1, Nanjing, Jiangsu, China) was also determined in the cultured neurons. The level of the oxidants or the activities of these antioxidant enzymes were detected by specific colorimetric kits according to the manufacturer's instructions. Briefly, for the measurement of SOD activity and CAT activity, the OD readings of test samples were transformed into inhibited levels, based on the standard curves and calculated activities of SOD and CAT. For the measurement of GSH, the content of GSH of tested samples was determined based on the standard concentration of GSH.

2.6. DNA extraction and cDNA generation

Total DNA was extracted from 20 mg of tissue or 10^7 cultured neurons utilizing a Genomic DNA Purification kit (Tiangen Biotech Co., LTD, Beijing, China) according to the manufacturer's instructions. Total RNA was extracted from about 50 mg of tissue or 10^7 cultured neurons with an RNA extraction kit (Solar Bio, Beijing, China) according to the instructions. The purification and concentration of DNA and RNA were measured by a GeneQuant pro RNA/DNA Calculator (Biochrom, Cambridge, UK). The extracted RNA was stored at −80 °C until it was transcribed to cDNA with a PrimeScript RT reagent kit (TaKaRa, Dalian, China), and the purification and concentration were measured. The DNA and cDNA samples were aliquoted and stored at −20 °C until further use.

2.7. Quantification of mtDNA 4834-bp deletion

The level of mtDNA 4834-bp deletion was determined by TaqMan real-time polymerase chain reaction (PCR) assay. The copy number of the D-loop in mtDNA was used as a measurement of the total number of mtDNA copies in a given sample. Primers and probes for the D-loop and the 4834-bp deletion from the rat mitochondrial genome was described by Nicklas and colleagues previously [4]. PCR amplification was performed by using the Roche LightCycler 480 (LC480) real-time PCR system (Roche Diagnostics Ltd, Rotkreuz, Switzerland) in a 20-μl reaction mixture composed of 10 μl of a 2x TaqMan PCR mix (TaKaRa, Dalian, China), 0.2 μl of each probe (10 mM), 0.4 μl of each reverse and forward primer (10 mM), 5 μl of distilled water and 4 μl of the sample DNA, with each reaction mixture containing 40–50 ng DNA. The amplification conditions and the calculation method were described in our previous work [34].

2.8. Nissl staining analysis

The Nissl staining analysis was performed according to our published paper with few modifications [33]. Briefly, serial transverse sections made from paraffin-embedded brains were dewaxed with xylene, followed by rehydration in graded alcohol and immersion in 0.3% toluidine blue for 40 min at 60 °C. The number of neurons in the V layer of the auditory cortex was counted in accordance with our previous criterion [33].

2.9. Western blot analysis

2.9.1. Protein extraction

Tissues from the auditory cortex were lysed immediately with a radioimmunoprecipitation assay (RIPA) Lysis Solution (Beyotime, Haimen, China), which contains a cocktail of phosphatase inhibitors as well as phenylmethylsulfonyl fluoride (PMSF), at a ratio of 200 μl of lysis buffer per 20 mg tissue. Cultured neurons grown on a 12-well plate were washed with cold phosphate-buffered saline (PBS) and then lysed with the same RIPA Lysis Solution as above, with 100 μl of lysis buffer used per well. The following procedures were performed according to the manufacturer's instructions. After the protein concentration was determined with an enhanced Bicinchoninic Acid (BCA) Protein Assay Kit (Beyotime, Haimen, China), 5x sodium dodecyl sulfate-polyacrylamide gel electrophoresis (SDS-PAGE) loading buffer (Beyotime, Haimen, China) was added to the remaining lysate, followed by heating at 95 °C for 10 min.

2.9.2. SDS-PAGE analysis

Equal amounts of protein were loaded onto 10% SDS-polyacrylamide gels for electrophoresis. The following processes were performed as previously described in our laboratory [33]. Detailed information for the primary antibodies used are listed in the following table:

Peptide/Protein Target	Name of Antibody	Manufacturer; Catalog No.	Host Species, Monoclonal or Polyclonal	Dilution
Actin	Anti-beta-actin monoclonal antibody	Lianke; Mab1445	Mouse monoclonal	1:3000
GRP78	GRP78 antibody	GeneTex GTX102580	Rabbit polyclonal	1:2000
HSP90 alpha	HSP90 alpha antibody	GeneTex GTX109753	Rabbit polyclonal	1:2000
Peroxiredoxin 2	Peroxiredoxin 2 polyclonal antibody	Proteintech 10545-2-AP	Rabbit Polyclonal	1:1000
TXNRD1	TXNRD1 Polyclonal antibody	Proteintech 11117-1-AP	Rabbit polyclonal	1:1000
DNA polymerase γ	DNA polymerase γ antibody	Bioss Bs-13017R	Rabbit Polyclonal	1:500
OGG-1	Anti-OGG1	Abcam ab1776	Rabbit	1:500
Lamin B1	Lamin B1 polyclonal antibody	Proteintech 12987-1-AP	Rabbit	1:2000
Lamin A/C	Anti-lamin A/C rabbit antibody	Wanleibio WL0457b	Rabbit	1:3000
Phospho-PI3 kinase p85 (Tyr-458)/p55 (Tyr-199) antibody	Phospho-PI3 kinase p85 (Tyr458)/p55 (Tyr199)	Cell Signaling Technology; 4228	Rabbit polyclonal	1:1000
PI3K	P85;PI3R1 monoclonal antibody	Proteintech; 60225-1-Ig	Mouse monoclonal	1:1000
AKT (phospho Ser-473)	AKT1 phospho (pS473) Rabbit monoclonal antibody	Epitomics; 2118-1	Rabbit monoclonal	1:1000
AKT	AKT 1 + 2 + 3 antibody	GeneTex; GTX121937	Rabbit polyclonal	1:4000
phospho-AMPK (Thr-172)	p-AMPKα1/2 Antibody	Santa Cruz Biotechnology; sc-33524	Rabbit polyclonal	1:600
AMPKα1/α2	AMPKα1/AMPKα2 (ab-174/ab-172) antibody	Signalway Antibody; 21191	Rabbit polyclonal	1:1000
VDAC1	VDAC1 antibody	GeneTex; GTX114187	Rabbit polyclonal	1:3000
OXPHOS	Anti-Rt/Ms Total Oxphos Complex Kit	Life Technologies 45-8099	Mouse monoclonal	1:1000

2.10. Flow cytometry

2.10.1. Detection of apoptosis by Annexin V/propidium iodide (PI)

Annexin V-FITC/PI double labeling apoptosis kit (KeyGEN BioTECH, Nanjing, Jiangsu, China) was utilized to evaluate apoptosis in cultured neurons. Briefly, after each treatment, cells were rinsed twice with cold PBS and incubated with EDTA-free 0.25% trypsin at 37 °C until 80% of the cells were detached. Cell suspensions were collected and centrifuged at 1000 rpm for 5 min. The supernatant was discarded, and cold PBS was used to wash the pellets two times. The cells (1×10^6) were resuspended in 500 μl of 1× binding buffer containing 5 μl of annexin V-FITC and 5 μl PI, incubated for 15 min at room temperature in the dark and then analyzed by flow cytometry (FACSCalibur, BD Biosciences, Carlsbad, CA, USA). About 10 μl the remaining labeled cell suspension was dropped on a coverslip and monitored under a fluorescence microscope for nuclear changes.

2.10.2. Determination of ΔΨm

Determination of ΔΨm was performed using flow cytometry. Changes in ΔΨm were detected using Mitochondrial Membrane Potential Assay Kit with JC-1 (C2006, Beyotime, Haimen, China) according to the manufacturer's instructions.

2.11. Analysis of ATP production

An ATP Assay Kit (S0026, Beyotime, Haimen, China) was used to determine the content of ATP in cultured neurons according to the manufacturer's instructions. The chemiluminescence signal was read with a multi-mode microplate reader (BioTek Instruments, Winooski, VT, USA).

2.12. Analysis of ROS production

The intracellular ROS level was detected using 2′, 7′-dichlorofluorescein diacetate (DCFH-DA; S0033, Beyotime, Haimen, China), an oxidation-sensitive fluorescent probe. Cells were seeded into 24-well plates (5×10^5 cells/well). After treatments for the indicated amount of time, the cells were then incubated with DCFH-DA (10 μM) for 30 mins at 37 °C, followed by 3 washes of the cells with serum-free DMEM and measurement with a multi-mode microplate reader ($\lambda_{ex}=488$ nm, $\lambda_{em}=525$ nm).

2.13. Statistical analysis

All data are expressed as mean ± SD. Analyses were performed using the Statistical Package for the Social Sciences (SPSS) 11.5 (SPSS Inc., Chicago, IL, USA). Hypothesis testing was performed using one-way analysis of variance (ANOVA) except when otherwise stated. The least significant difference post hoc test was used to compare differences among subgroups. Differences with $P < 0.05$ were considered to be statistically significant. All experiments were repeated at least three times, and all statistical tests were two sided.

3. Results

3.1. Exogenous H_2S attenuates oxidative stress in mimetic aging model via CaMKKβ/AMPK and PI3K/AKT signaling pathways

D-gal is widely used as an inducer of mimetic aging due to its metabolic toxicity and oxidative damage [35]. In this study, we established a mimetic aging model *in vivo* and *in vitro* using D-gal treatment. We also studied the effect of NaHS, the commonly used H_2S donor, on the development of aging at different times after D-gal injection (mimetic aging rats at 3 months and 9 months of age).

3.1.1. NaHS activates AMPK and PI3K/AKT signaling pathways in vivo and in vitro

CaMKKβ plays an important role in calcium signal transduction in neurons and mediates multiple functions by activating AMPK, such as cell cycle regulation [36] and energy balance control [37]. As

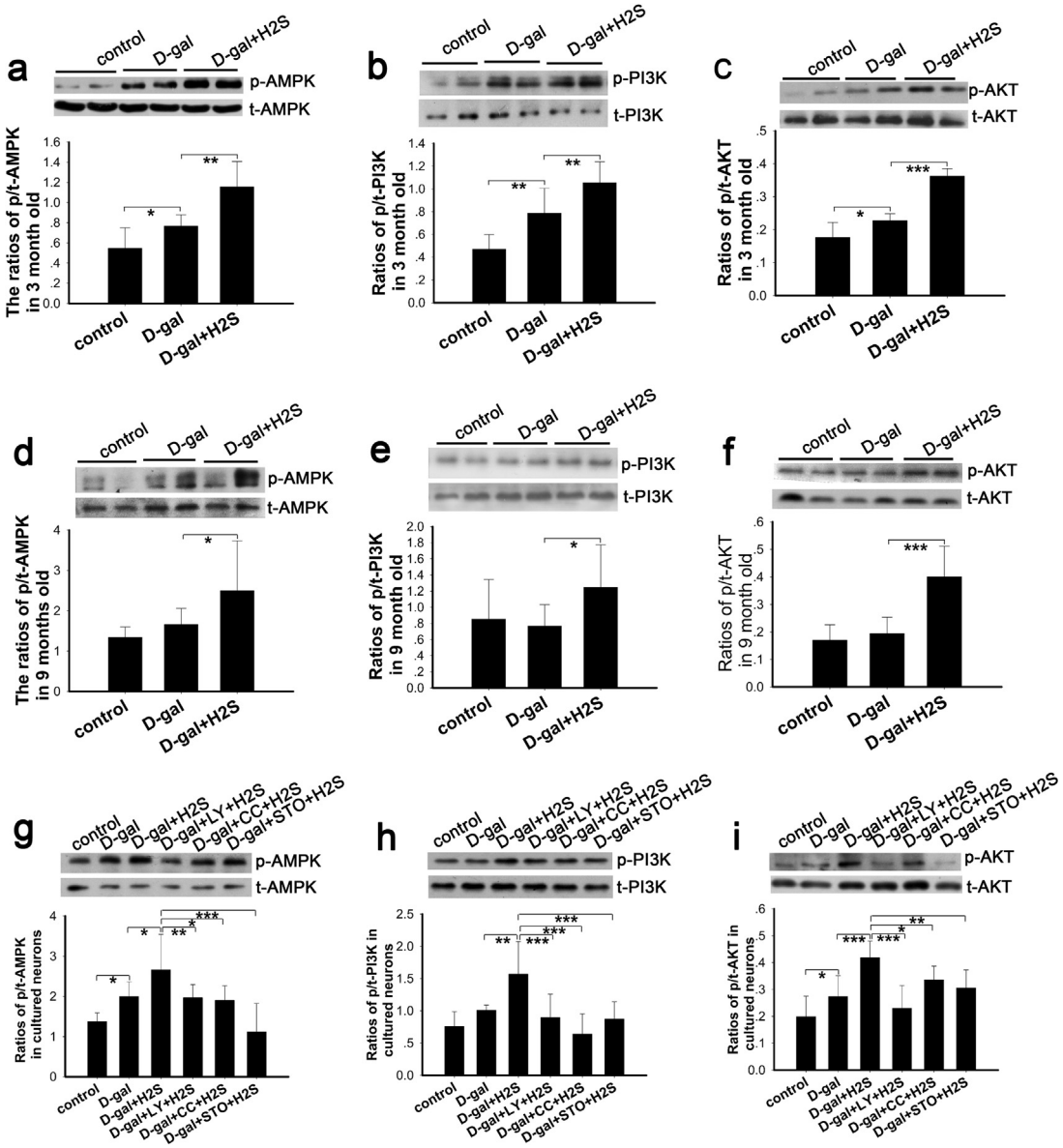

Fig. 1. Western blot analysis of the effects of NaHS on the PI3K/AKT and CaMKKβ/AMPK signaling pathways in mimetic aging. NaHS affects AMPK, PI3K and AKT phosphorylation levels in mimetic aging rats of 3 months (a-c) and 9 months (d-i) of age as well as cultured neurons; STO-609, LY-294002 and compound C inhibited the phosphorylation of AMPK, PI3K and AKT *in vitro* (g-i). * $p < 0.05$, ** $p < 0.01$, *** $p < 0.001$. The data are presented as mean ± SD. N = 6 for each subgroup.

summarized by Morales et al., reactive oxygen and nitrogen species activate AMPK by CaMKKβ [38]. PI3K/AKT play a key role in regulating apoptosis and the cell cycle [39]. To explore changes in the activity of CaMKKβ/AMPK and PI3K/AKT pathways in D-gal-induced mimetic aging and identify whether these pathways mediate the function of H_2S on aging, we evaluated the phosphorylation levels of AMPK, PI3K and AKT by western blot. Activation of CaMKKβ is regulated by its autoinhibitory domain but not by direct phosphorylation of residues [40]; therefore, we did not detect the phosphorylation level of CaMKKβ by western blot. Our data demonstrated that in the 3-month-old rats (Fig. 1a, b, c), the phosphorylation level of AMPK was significantly increased in the mimetic aging rats, and AMPK phosphorylation was upregulated further in the NaHS-treated group, as compared with the mimetic aging group (Fig. 1a). There was a significant change in the PI3K phosphorylation level in the mimetic aging group compared with the control group; meanwhile, NaHS enhanced the phosphorylation level of PI3K when compared with the mimetic aging group (Fig. 1b). Phosphorylation of AKT was increased in the mimetic aging group and increased further in the NaHS-treated group, as compared with the control group and the D-gal-treated group, respectively (Fig. 1c). Unlike the 3-month-old rats, phosphorylation of AMPK, PI3K and AKT in the 9-month-old D-gal-treated rats was not significantly different from the control group (Fig. 1d, e, f). Nevertheless, NaHS treatment markedly increased the phosphorylation levels of AMPK, PI3K and AKT (Fig. 1d, e, f). In the cultured neurons (Fig. 1g, h, i), phosphorylation levels of AMPK, PI3K and AKT were increased to differing degrees, and NaHS treatment dramatically enhanced their phosphorylation. To examine the effects of compound C and LY-294002 on the inhibition of AMPK phosphorylation and PI3K phosphorylation, respectively, two groups of D-gal-induced senescent neurons were treated with the inhibitors followed by treatment with NaHS. The results showed that the phosphorylation of AMPK, PI3K and AKT decreased (Fig. 1g, h, i). Next, we treated the senescent cells with STO-609, an inhibitor of CaMKKβ. The phosphorylation level of AMPK was decreased drastically (Fig. 1g), which suggests that AMPK activation is at least partially dependent on CaMKKβ activation.

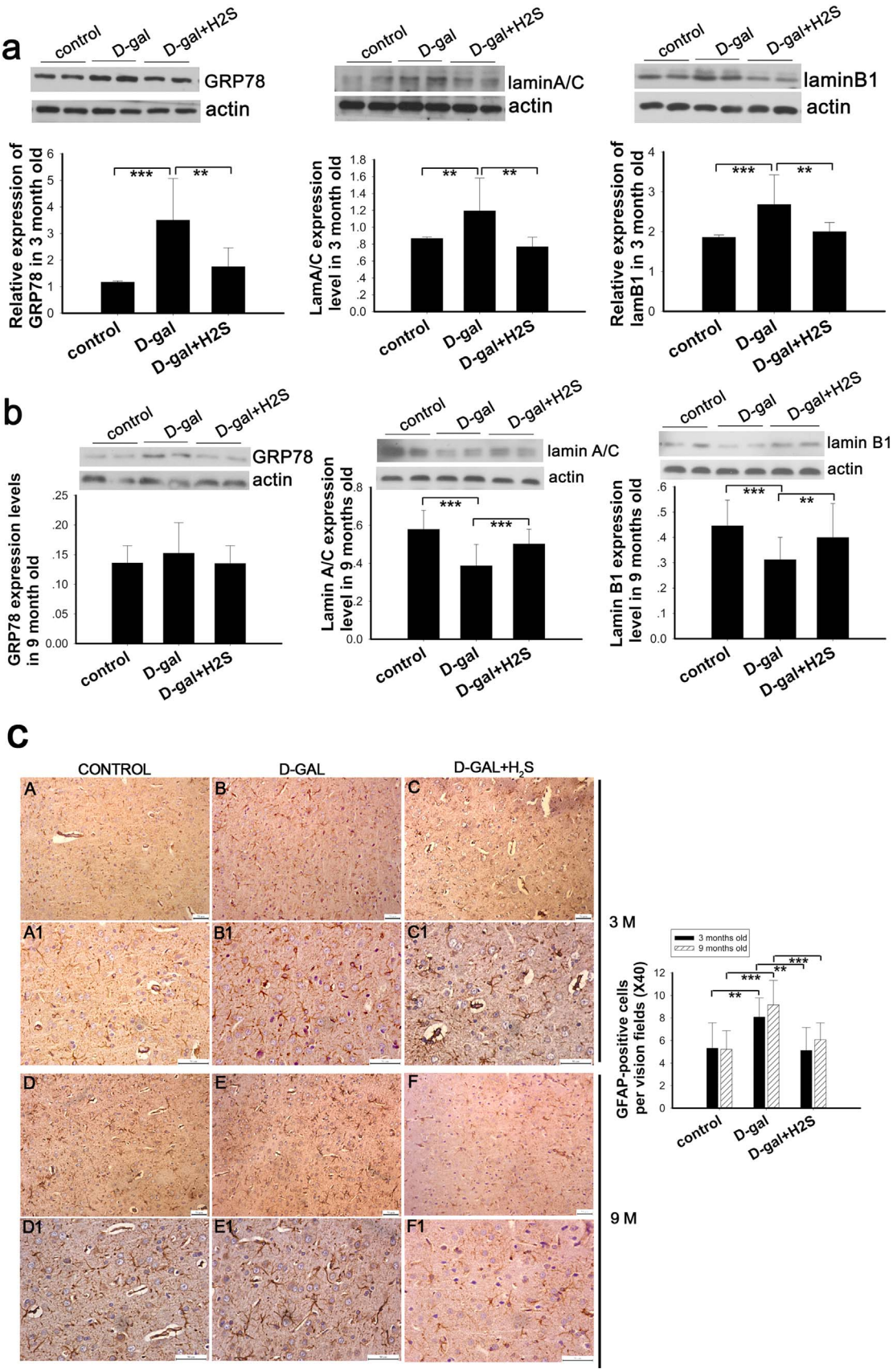

Fig. 2. Western blot analysis of oxidative stress and IHC analysis of astrogliosis in mimetic aging rats and the effect of NaHS on oxidative stress and astrogliosis. Oxidative stress was evaluated by expression of GRP78, lamin A/C and lamin B1 in 3-month-old and 9-month-old rats (a, b). Astrogliosis was evaluated by staining with GFAP in 3-month-old and 9-month-old rats (c). A1-C1 and D1-F1 were magnified from A-C and D-F, respectively. Number of GFP-positive cells were counted and displayed in the right statistical chart. ** $p < 0.01$, *** $p < 0.001$. The data are shown as mean ± SD. N = 6 for each subgroup.

3.1.2. NaHS decreases the oxidative stress level in mimetic aging rats

GRP78 is used to evaluate stress levels due to its key role in sensing endoplasmic reticulum stress and initiation of ER stress [41]. Lamin A/C and lamin B1 are key constituents of the lamina, which lines the inner nuclear membrane and determines its shape and integrity [42]. As reported by Barascu and coworker, oxidative stress increases the expression of lamin B1, and it acts as a general molecular mediator that controls oxidative stress-induced senescence [43]. In addition, astrocytes are activated in response to various pathophysiological processes in the central nervous system [44]. To evaluate the effect of NaHS on mimetic aging, we determined the expression level of GRP78, lamin B1 and lamin A/C by western blot and glial fibrillary acidic protein (GFAP) by IHC in the auditory cortex.

In our study, we found that GRP78, lamin B1 and lamin A/C were upregulated in the D-gal-treated rats at 3 months of age (Fig. 2a), and NaHS decreased their expression significantly (Fig. 2a). We also measured the expression levels of GRP78, lamin B1 and lamin A/C in the 9-month-old rats. The data showed that GRP78 expression is increased in the mimetic aging group but decreased in the NaHS-treated group; however, these changes were small and not statistically significant (Fig. 2b). To our surprise, the expression of lamin B1 and lamin A/C was decreased in the D-gal-induced mimetic aging rats (Fig. 2b), which differed from the 3-month-old mimetic aging rats. Furthermore, NaHS increased the expression level of lamin B1 and lamin A/C in the 9-month-old mimetic aging rats (Fig. 2b). Our results also showed that GFAP expression is increased in the mimetic aging rats, while NaHS reversed this increase (Fig. 2c).

3.1.3. NaHS decreased the oxidative stress level in cultured neurons mediated by CaMKKβ/AMPK and PI3K/AKT pathways

To investigate how NaHS affects the development of aging by regulation of the CaMKKβ/AMPK and PI3K/AKT pathways, we used *in vitro* mimetic senescent neurons, which were induced by D-gal for further experiments.

The cultured neurons were treated with increasing concentrations of D-gal (0–16 mg/ml) for 7 days and then cell viability was evaluated by CCK-8 kit and by β-galactosidase staining. The cellular activity of neurons treated with D-gal changed with the different concentrations, exhibiting a decreasing pattern that was statistically significant at 10 mg/ml (Fig. 3a). We also observed the cultured neurons under a standard optical microscope to identify the growth state and found good growth at the 7th day after seeding and day 14 (the 7th day after D-gal treatment) (Fig. 3b). The neurons were also evaluated by β-galactosidase staining, which showed that the number of positively stained cells increased with the increasing concentration of D-gal (Fig. 3c). The number of positive cells increased significantly at the 4-mg/ml concentration and showed a tendency to increase as the concentration of D-gal increased above 4 mg/ml. According to these results, we successfully established a senescent cell model, and we utilized 8 mg/ml of D-gal to induce the senescence of neurons for the subsequent experiments.

Expression levels of GRP78, lamin A/C and lamin B1 were determined by western blot to evaluate the level of oxidative stress in cultured neurons. Our data demonstrated that the expression levels of GRP78, lamin A/C and lamin B1 were increased in the D-gal-induced senescent group (Fig. 3e, f, g). Meanwhile, the expression levels of GRP78, lamin A/C and lamin B1 were decreased in the NaHS-treated senescent group. Conversely, in the groups pretreated with LY294002, compound C and STO-609, NaHS did not decrease the expression of GRP78, lamin A/C and lamin B1 (Fig. 3e, f, g), which suggested a higher level of oxidative stress in these three groups. To confirm the oxidative stress level in each group, we acutely measured the level of ROS. As our data suggests, ROS production was increased by D-gal and decreased by NaHS treatment; furthermore, inhibition of PI3K, AMPK and CaMKKβ phosphorylation increased ROS production (Fig. 3h). This observation is in agreement with the expression of the oxidative stress markers.

3.2. NaHS decreased apoptosis through CaMKKβ/AMPK and PI3K/AKT

We studied the effect of NaHS on apoptosis and pathways involved in mediating the regulation of apoptosis. We analyzed apoptosis by detecting caspase-3, counting the number of neurons stained by toluidine blue in the auditory cortex and annexin V/PI staining *in vitro*. In the 3-month-old rats, the D-gal-induced mimetic aging rats showed more apoptotic cells and reduced numbers of neurons compared with the control group. NaHS administration decreased apoptosis (Fig. 4a) and slightly reversed the reduction of neurons (not statistically significant; Fig. 4e). A similar change was observed in the 9-month-old rats except that NaHS did not attenuate the reduction of neurons (Fig. 4b, e). We also detected apoptosis *in vitro* by staining with annexin V/PI (Fig. 4c), and we summed the percentage of cells in the upper left (UL), upper right (UR) and lower right (LR) panels as the total percentage of apoptotic cells. These results demonstrated that D-gal treatment increased the apoptosis of neurons and that NaHS attenuated this apoptosis. However, the anti-apoptotic activity of NaHS was decreased in the groups where the phosphorylation of PI3K, AMPK and CaMKKβ were inhibited. To observe nuclear changes, we also observed neurons after staining with annexin V/PI. A similar change in apoptosis was observed under a fluorescence microscope though the nucleus was not noticeably changed (Fig. 4d). In conclusion, exogenous H_2S alleviated apoptosis *in vivo* and *in vitro* through the CaMKKβ/AMPK and PI3K/AKT pathways.

3.3. NaHS increased activity of antioxidant through CaMKKβ/AMPK and PI3K/AKT

A previous study has demonstrated that under normal conditions, ROS produced by the mitochondria are easily metabolized or scavenged by endogenous antioxidant mechanisms [45], such as GSH, CAT and SOD, so that the organism or cells maintain homeostasis. However, the aging process affects this homeostasis. We examined the activity and expression of antioxidants in aging models and investigated the effect of NaHS on antioxidants. The activity of GSH and SOD was detected in the rats' serum as a reflection of overall activity. In cultured neurons, the intracellular activity of GSH and SOD was measured. The results suggest that GSH and SOD were decreased in the aging model and increased upon treatment with NaHS (Fig. 5a, b). In the *in vitro* study, inhibition of PI3K, AMPK and CaMKKβ blocked the effects mediated by NaHS (Fig. 5a, b). We also detected the activity of CAT, a marker of peroxisomes, in cultured neurons. CAT activity was decreased dramatically in senescent cells and was upregulated by NaHS; however, this upregulation was eliminated significantly by inhibitors of PI3K, AMPK and CaMKKβ. Peroxiredoxin 2 (PRDX2) is a member of the peroxiredoxin family of antioxidant enzymes and is expressed in the neurons of the central nervous system [46]. Thioredoxin reductase 1 (TXNRD1) belongs to the thioredoxin system, which is crucial for cellular function, cell proliferation and antioxidant defense [47], and is expressed in the cytoplasm of neurons in rats' central nervous system [46]. As determined by western blot in our study, PRDX2 and TXNRD1 were decreased in the D-gal-induced aging model *in vivo* and *in vitro* (Fig. 5d, e). These changes were reversed by NaHS, while PI3K, AMPK and CaMKKβ inhibitors suppressed these effects (Fig. 5d, e). These observations demonstrated that NaHS enhanced the antioxidant activity *via* CaMKKβ/AMPK and PI3K/AKT pathways.

3.4. NaHS protects mitochondria through CaMKKβ/AMPK and PI3K/AKT pathways

It was reported that H_2S produces beneficial effects on mitochondrial function [48]; nevertheless, the related signaling pathways still remain unclear. In our study, we evaluated the function of mitochon-

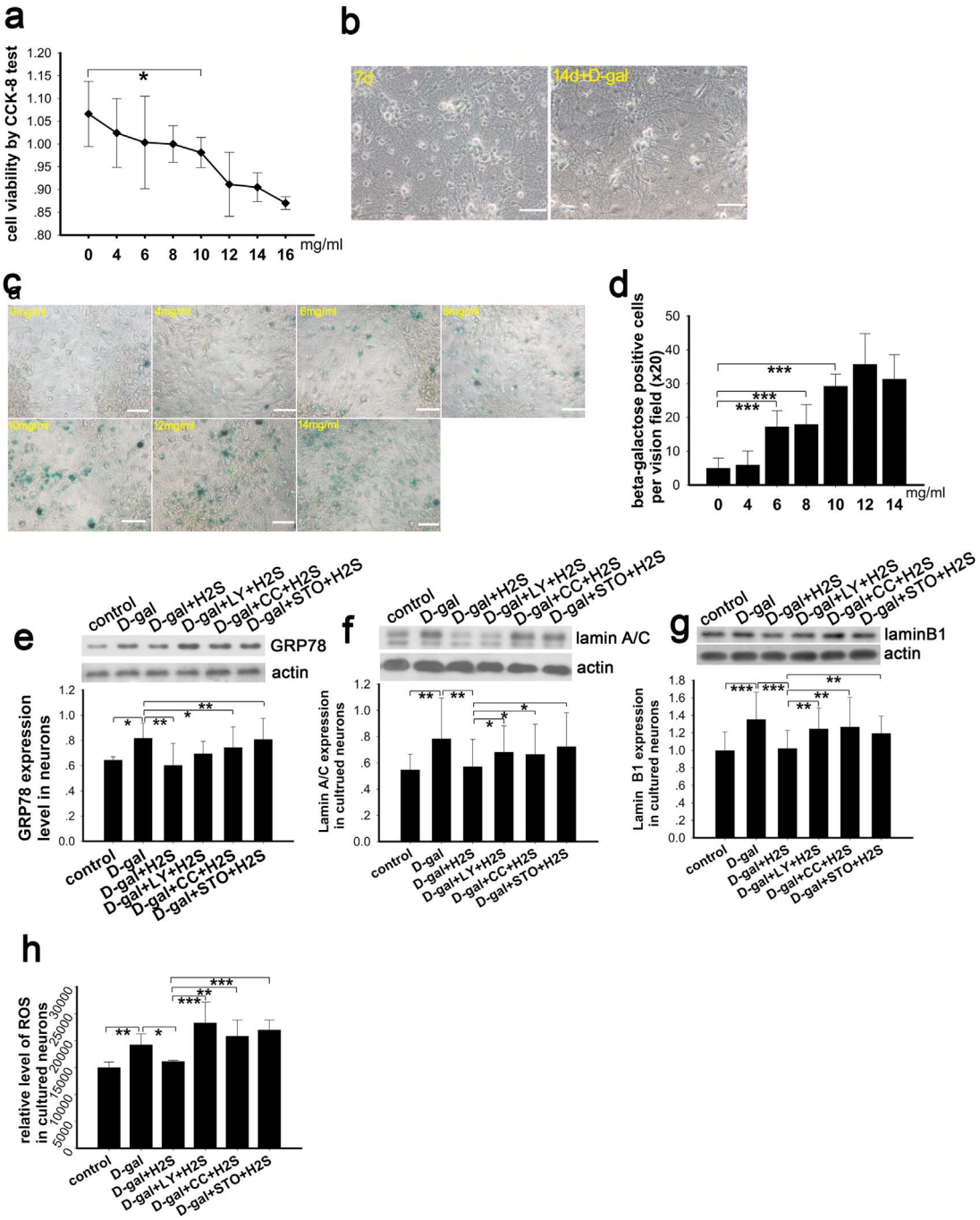

Fig. 3. Determination of senescence and oxidative stress levels in cultured neurons. Optimal concentration of D-gal was selected by CCK-8 test (a), N = 9 for each subgroup. Primary cultured neurons were observed after being seeded on a plate for 7 days and after D-gal treatment for 7 days (b). Senescence was evaluated by the Senescence β-Galactosidase Staining Kit in neurons treated with graded concentrations of D-gal (c). Positive cells for β-galactosidase staining were counted and shown in panel d, N = 9 for each subgroup. The oxidative stress level was evaluated by western blotting analysis of GRP78, lamin A/C and lamin B1 in senescent cells, cells treated with NaHS and cells treated with inhibitors of PI3K, AMPK and CaMKKβ (e-g), N = 6 for each subgroup. Generation of ROS in the cultured neurons was determined (h), N = 6 for each subgroup. Scale bar = 25 μm, $p < 0.05$, ** $p < 0.01$, *** $p < 0.001$. The data are displayed as mean ± SD.

dria by determining the expression of oxidative phosphorylation (OXPHOS) complexes, key constituents of the mitochondrial respiratory chain, detecting mitochondrial membrane potential and ATP production and exploring the relationship between the effect of H_2S on mitochondria and the CaMKKβ/AMPK and PI3K/AKT pathways. As suggested by our results, complex I and complex II expression was increased in the D-gal-induced mimetic aging rats at 3 months of age, while NaHS decreased the expression of complex I and complex II. The expression of complex V and complex III was stable across all groups of 3-month-old rats (Fig. 6a and Supplementary information Fig. S2). However, differing data were observed for the 9-month-old rats. The mimetic aging rats showed decreased expression of OXPHOS complexes, particularly complex I and complex II though they did not reach statistical significance. NaHS treatment mildly decreased the OXPHOS expression, which also was not statistically significant (Fig. 6b and Supplementary information Fig. S2). In the cultured neurons, the expression of OXPHOS complexes was increased after D-gal treatment, except for complex V. In agreement with the *in vivo* study, NaHS decreased the expression levels of complexes I-V to differing degrees (Fig. 6c and Supplementary information Fig. S2). To investigate

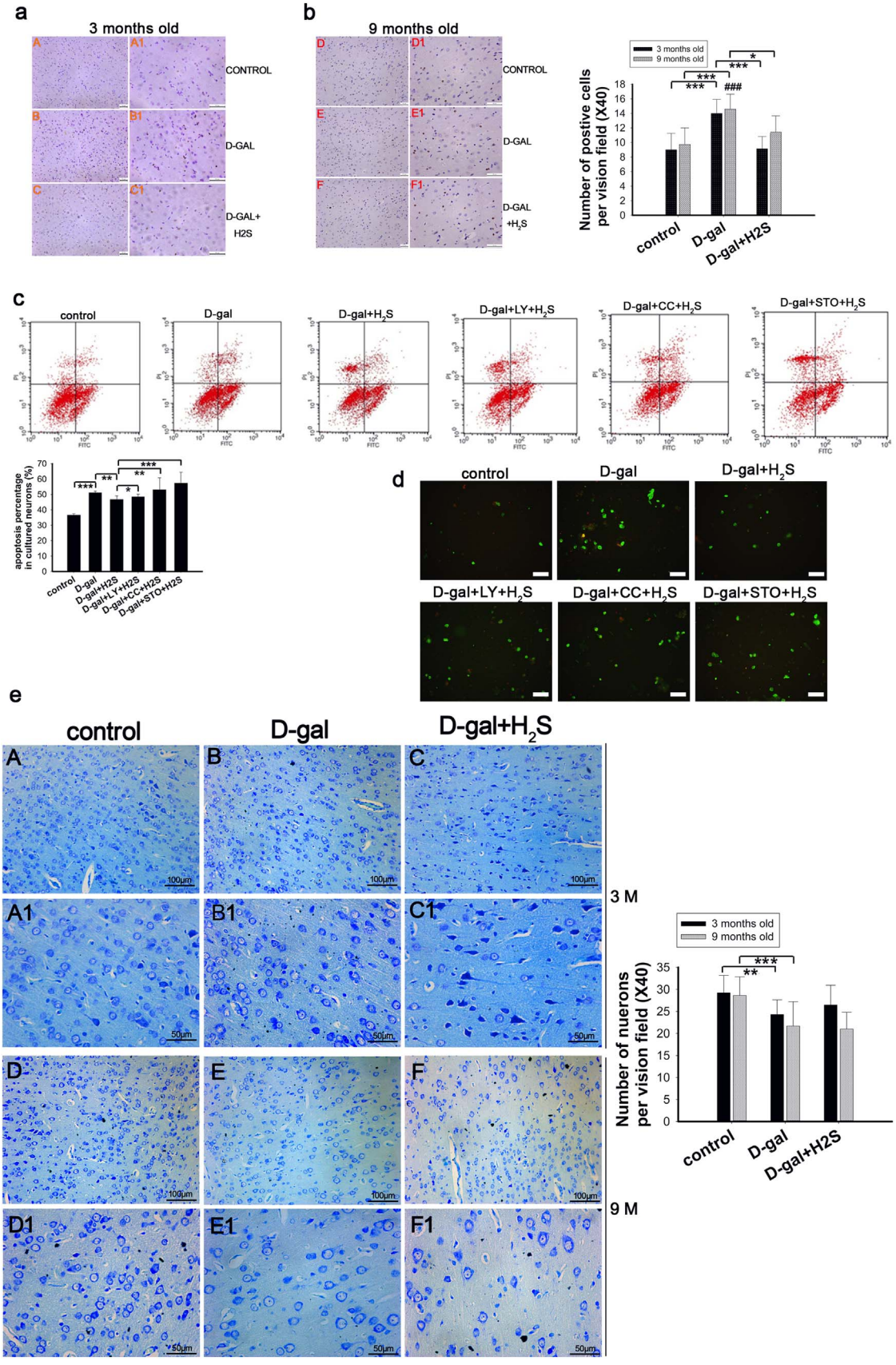

(caption on next page)

Fig. 4. Analysis of apoptosis *in vivo* and *in vitro*. Caspase-3 was evaluated by IHC in auditory cortex (a, b); the number of caspase-3 positive cells was counted and displayed in the right statistical graph. Apoptosis in cultured neurons was determined by flow cytometry (c). LL (lower left) shows the neurons stained annexin V (-) and PI (-), indicating viable cells. Nonviable cells include the following: UL (upper left) shows the neurons stained annexin V (-) and PI (+), which are necrotic cells; UR (upper right) shows annexin V (+) and PI (+) staining that are the late apoptotic cells; and LR (low right) shows annexin V (+) and PI (-) staining, which are the early apoptotic cells. Percentages of UL, UR and LR panels were summed as the total percentage of apoptotic cells. Cells digested from plates were observed by fluorescence microscopy after staining with annexin V/PI (d). Sections from auditory cortex of rats were stained with toluidine blue and used to count surviving neurons. A1-C1 and D1-F1 were magnified from A-C and D-F, respectively, with the corresponding statistical chart displayed on the right (e). * $p < 0.05$, ** $p < 0.01$, *** $p < 0.001$. The data are displayed as mean ± SD. N = 6 for each subgroup.

whether the signaling pathways of CaMKKβ/AMPK and PI3K/AKT were involved in the regulation of OXPHOS by NaHS, we inhibited PI3K, AMPK and CaMKKβ prior to the NaHS treatment in the senescent cells. The results demonstrated that the expression levels of complexes I-IV, particularly complex I and complex II, were increased compared with the non-inhibited group (Fig. 6c and Supplementary information Fig. S2). The above observations suggested that the OXPHOS expression was changed by oxidative stress and during aging, and NaHS decreased the expression of OXPHOS. To determine whether mitochondrial function was changed, we examined the ΔΨm by flow cytometry to detect early apoptotic mitochondria that harbor decreased ΔΨm. The data showed that the number of abnormal mitochondria was increased in the D-gal treatment group. NaHS treatment decreased the number of abnormal mitochondria, but this effect was prevented by inhibiting PI3K, AMPK

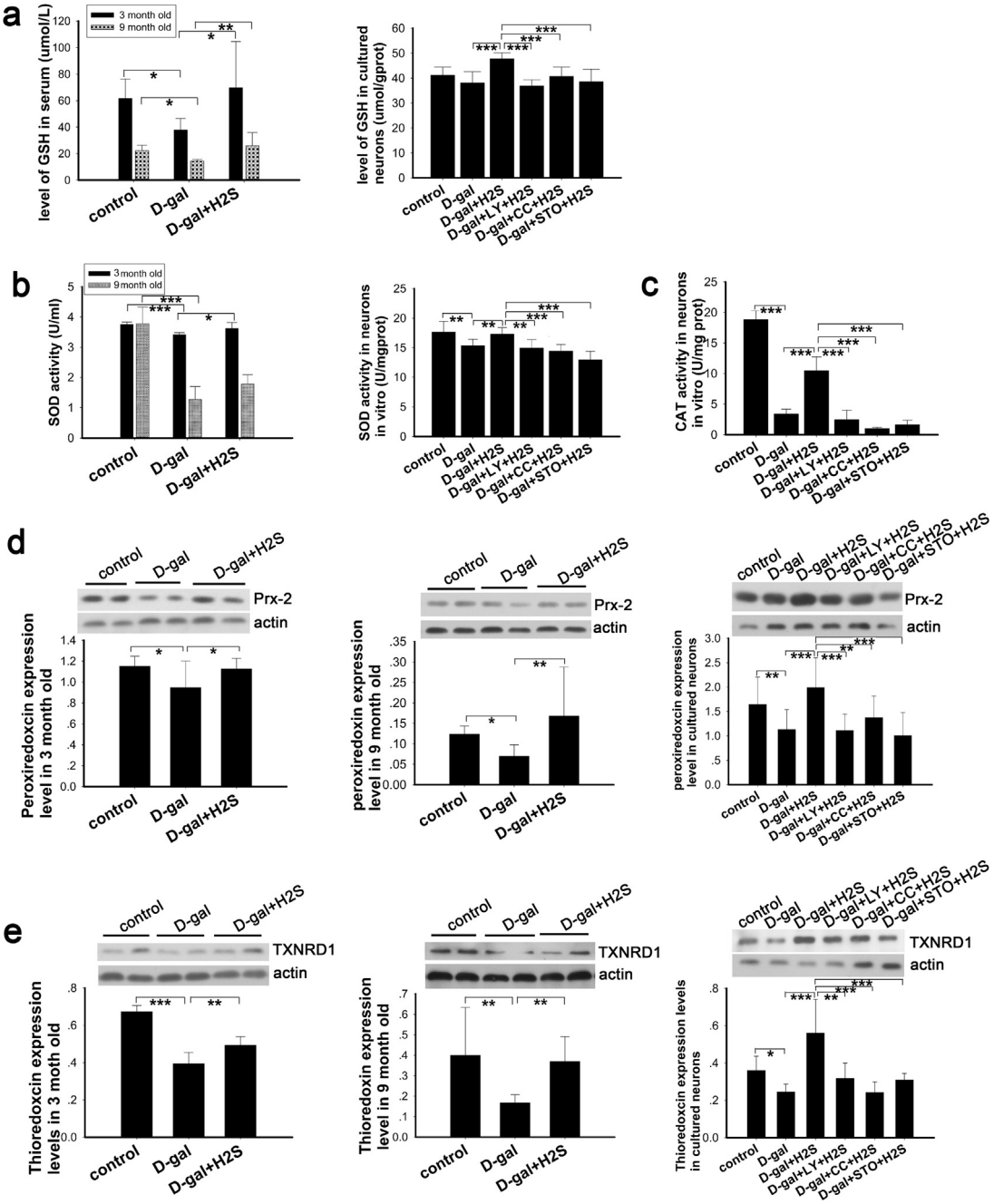

Fig. 5. Analysis of antioxidants *in vivo* and *in vitro*. Activity of serous and intracellular GSH (a) and SOD (b) were evaluated in rats and cultured neurons, respectively, N = 8 for each subgroup. Activity of intracellular CAT was tested in cultured neurons (c), N = 5 for each subgroup. Expression of antioxidant enzymes was determined by western blot analysis in the auditory cortex of rats and cultured neurons (d, e), N = 6 for each subgroup. * $p < 0.05$, ** $p < 0.01$, *** $p < 0.001$. The data are presented as mean ± SD.

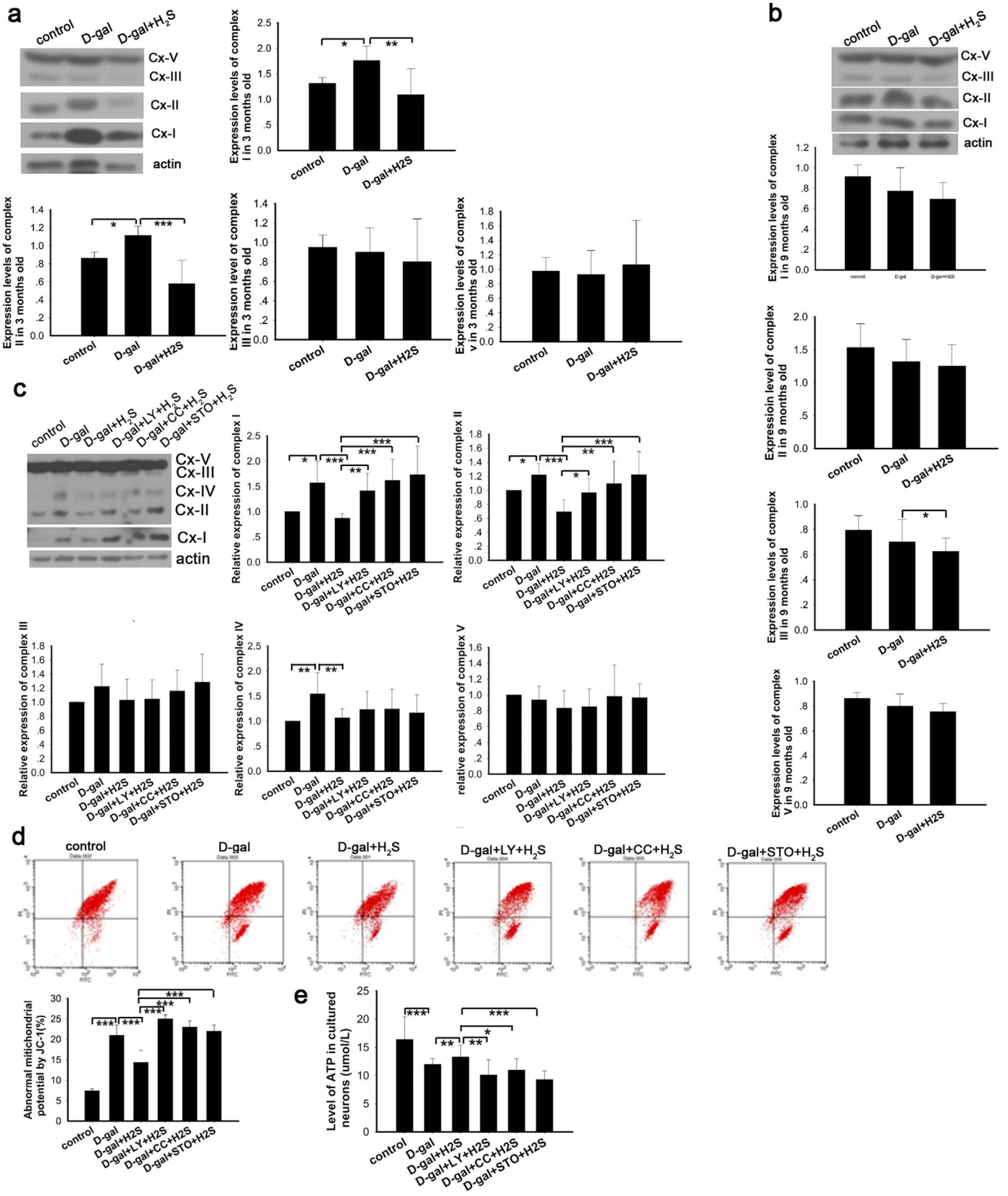

Fig. 6. Evaluation of protection by NaHS on mitochondria *in vivo* and *in vitro*. Expression of OXPHOS in rats (a, b) and cultured neurons (c) was determined by western blot analysis. Mitochondrial potential was evaluated by JC-1 staining with flow cytometry. X-axis indicates green channel and Y-axis indicates red channel. Normal mitochondrial potential showed higher red intensity and abnormal mitochondrial potential displayed higher green intensity after staining with JC-1. The LR area was calculated as abnormal mitochondrial potential (d). ATP production in cultured neurons in each group was determined (e). * $p < 0.05$, ** $p < 0.01$, *** $p < 0.001$. The data are exhibited as mean ± SD. N = 6 for each subgroup.

and CaMKKβ (Fig. 6d). In addition, the mitochondrion produces ATP, and ATP production is a direct indicator of mitochondria function. Our data showed that NaHS protected mitochondria from D-gal-induced decreases in ATP levels. Additionally, the protection was blocked by inhibition of PI3K, AMPK and CaMKKβ (Fig. 6e). These data suggest that the protection of mitochondria occurs *via* the CaMKKβ/AMPK and PI3K/AKT pathways.

3.5. NaHS increased the expression of mtDNA repair enzymes by CaMKKβ/AMPK and PI3K/AKT

As is well known, oxidative stress results in both nuclear DNA damage and mtDNA damage when the equilibrium between the antioxidant systems and ROS production is perturbed. Under these conditions, mtDNA molecules are likely to be more susceptible to oxidized DNA damage [49]. Abnormalities in the fidelity and efficiency of mitochondrial DNA repair are likely related to DNA damage accumulation and aging. Base excision repair (BER) is the primary repair pathway in the mitochondria [50]. DNA polymerase gamma (DNA POLG) and 8-oxoG DNA glycosylase 1 (OGG-1) are the major repair enzymes in mitochondria [51,52]. In this study, we determined the expression level of DNA POLG and OGG-1 by western blot. The results demonstrated that DNA POLG was increased slightly in 3-month-old mimetic aging rats (Fig. 7a), while the expression of DNA POLG was decreased in 9-month-old rats compared with the control group (Fig. 7b). In the cultured neurons, DNA POLG was increased in the D-gal-induced senescent cells. NaHS increased the expression of DNA POLG in the 3- and 9-month-old rats and the cultured neurons (Fig. 7a, b, c). Nevertheless, the expression of DNA POLG was not increased in the groups inhibited by LY-294002, compound C and STO-609 (Fig. 7c). Similar to DNA POLG, the expression of OGG-1 was not significantly changed in the 3-month-old rats and was decreased in the 9-month-old rats, with the upregulation of OGG-1 blocked by the inhibitors (Fig. 7d, e, f). These results indicate that the capability of BER was changed in each group to differing degrees. Thus, we then detected the mtDNA common deletion (CD), a hallmark of aging and usually a result of oxidative damage [53,54], by TaqMan real-time PCR. These data demonstrated that D-gal-induced mimetic aging harbored an increased level of CD *in vitro* and *in vivo,* which was in agreement with our previous study [5] (Fig. 7g, h, i). In this study, NaHS significantly ameliorated the damage to mtDNA in 3-month-old rats, while slight ameliorations were observed in the 9-month-old rats and the cultured neurons that were not statistically significant (Fig. 7g, h, i). Thus, we did not evaluate the CD in groups treated with the LY-294002,

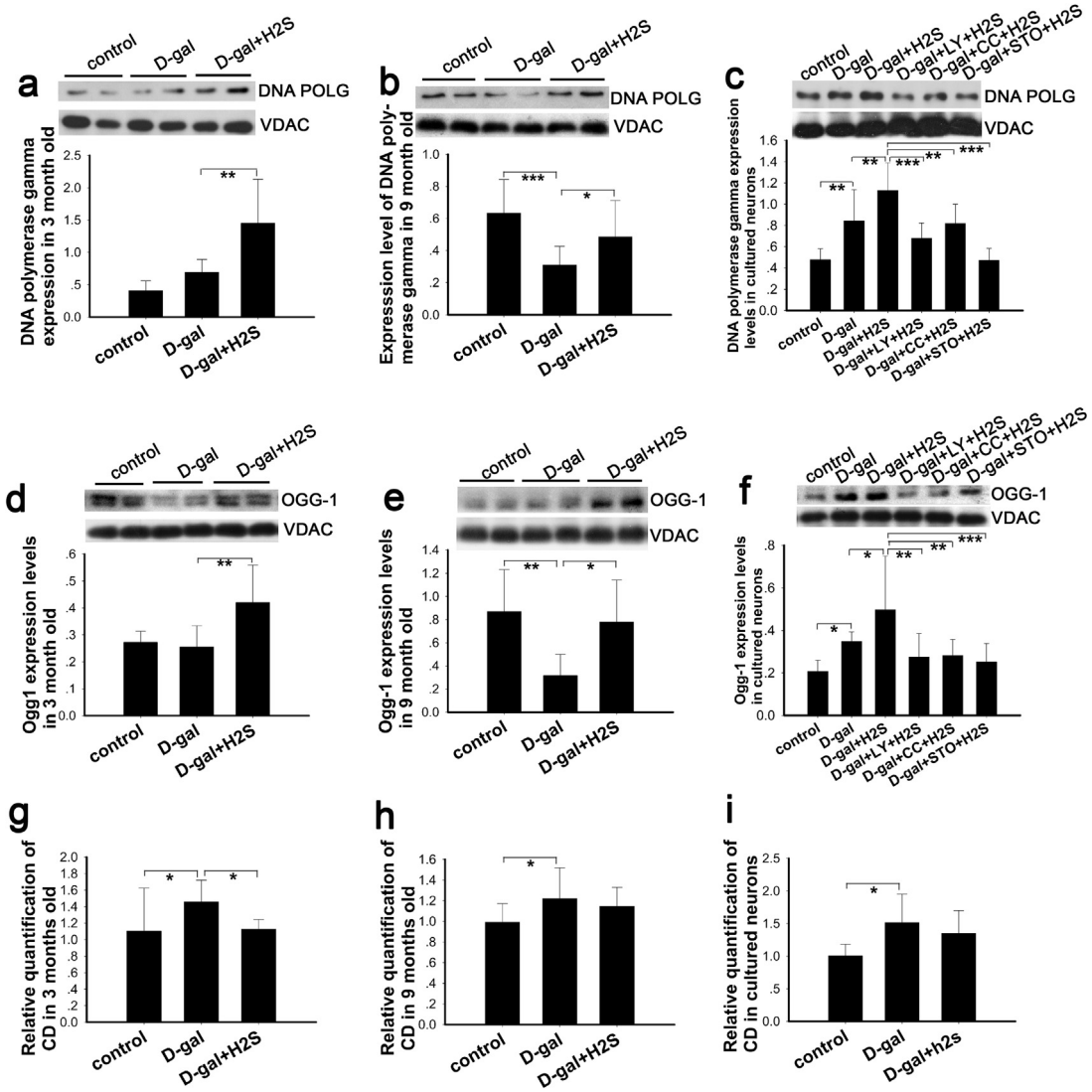

Fig. 7. Effect of NaHS on mitochondrial repair and deletion. Expression of DNA POLG and OGG-1 in mitochondria was evaluated by western blot analysis in rats (a, b, d, e) and in cultured neurons (c, f). Occurrence of CD in auditory cortex (g, h) and cultured neurons (i) was evaluated by real-time PCR. * $p < 0.05$, ** $p < 0.01$, *** $p < 0.001$. The data are exhibited as mean ± SD. N = 6 for each subgroup.

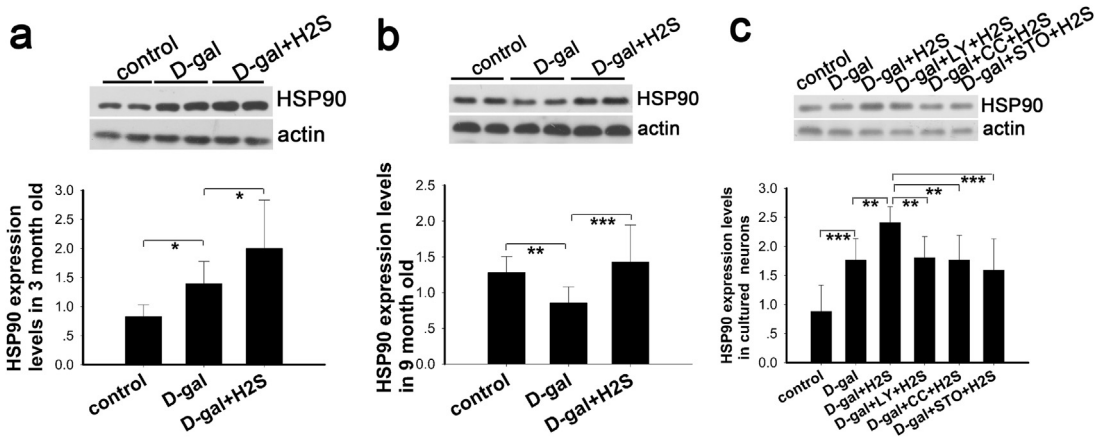

Fig. 8. Evaluation of NaHS on protein homeostasis indicated by HSP90 *in vivo* and *in vitro*. Expression of HSP90 alpha was determined by western blot analysis in auditory cortex of 3-month-old rats (a) and 9-month-old rats (b) as well as in cultured neurons (c). * $p < 0.05$, ** $p < 0.01$, *** $p < 0.001$. The data are displayed as mean ± SD. N = 6 for each subgroup.

compound C and STO-609 inhibitors.

3.6. NaHS improves molecular chaperone expression via CaMKKβ/AMPK and PI3K/AKT pathways

The capacity of the protein homeostasis (proteostasis) network declines during aging, facilitating neurodegeneration and other age-related diseases associated with protein aggregation [55]. Heat shock protein 90 (HSP90) not only supports protein folding but also the conformational maturation and maintenance of various medically relevant signaling proteins [56]. There are 2 major cytosolic HSP90 proteins, HSP90AA1, an inducible form, and HSP90AB1, a constitutive form. Other HSP90 proteins are found in the endoplasmic reticulum (HSP90B1) and mitochondria (TRAP1) [57]. We determined the expression of HSP90 alpha (cytosolic) and TRAP1 by western blot. Our study demonstrated that HSP90 expression increased in the D-gal-treated group, and the expression was further upregulated in the group treated with NaHS in the 3-month-old rats (Fig. 8a). Conversely, the expression of HSP90 was downregulated in the 9-month-old mimetic aging rats; whereas, this downregulation was reversed by NaHS (Fig. 8b). In the *in vitro* study, the expression level of HSP90 displayed a similar pattern as the 3-month-old rats. In addition, the increase in HSP90 expression was eliminated by LY-294002, compound C and STO-609 treatment. In our study, the expression of TRAP1 did not change significantly *in vivo* and *in vitro* in the D-gal-treated groups (data not shown). These results indicated that HSP90 alpha might be intimately related with aging and that NaHS affected the expression of HSP90 alpha *via* the CaMKKβ/AMPK and PI3K/AKT pathways.

4. Discussion

4.1. NaHS postponed the process of aging

Our study suggested that expression of GRP78, lamin B1 and lamin A/C were increased in the D-gal-treated group of 3-month-old rats (Fig. 2a) and cultured neurons (Fig. 3e, f, g), indicating an increased oxidative stress level. Conversely, in the 9-month-old rats, lamin B1 and lamin A/C expression were decreased significantly, while, interestingly, GRP78 expression was not prominently changed (Fig. 2b). As reported previously, the unfolded protein response, as mediated by molecular chaperones such as GRP78, was decreased in aged subjects, which showed increased susceptibility to ER stress than the young subjects [58]. Type A and B lamins are crucial for normal cellular function; in addition to DNA replication, transcription and chromatin organization, they are also involved in cell proliferation and differentiation and connection with the cytoskeleton, while abnormal expression of lamins leads to age-related cellular dysfunction [42]. In our study, the mimetic group of 3-month-old rats and the cultured neurons may suffer from increased oxidative stress as compared to the control group, with compensation by the upregulation of GRP78, lamin A/C and lamin B1. Conversely, the 9-month-old rats cannot handle persistent oxidative stress and displayed an aging phenotype. Our observation of GFAP expression (Fig. 2c) suggested a pathological process during aging. Reactive astrogliosis is a response of activated astrocytes found in many neurological diseases, such as trauma, neuroinflammation and neurodegeneration. Generally, astrogliosis can be regarded as a defensive reaction counteracting various stresses. However, this reaction can become maladaptive when it persists [44]. In addition, greater apoptosis and a larger reduction of neurons were observed in the D-gal treatment groups, as compared with the controls (Fig. 4). Moreover, both in the control rats and the mimetic aging rats, the apoptotic neuronal loss in the 9-month-old rats were slightly more frequent than in the 3-month-old rats. This observation is consistent with our previous studies showing that apoptosis, neuronal loss and neuronal damage are increased with age in both the mimetic aging models as well as the controls [5,34]. These data may mirror the pathogenesis of aging, which is tightly related with oxidative stress.

Our results suggest that NaHS decreased the expression of GRP78, lamin A/C and lamin B1 in 3-month-old rats (Fig. 2a). In the *in vitro* study (Fig. 3e, f, g), NaHS also decreased the production of ROS, as measured in the cultured neurons (Fig. 3h). Therefore, it was confirmed that NaHS functioned as a free radical scavenger and decreased oxidative stress. It has been reported that NaHS decreased the production of ROS dose-dependently in the kidney of Goto-Kakizaki (GK) diabetic rats. Moreover, the damage to the kidney was alleviated in the rats administered NaHS based on counting the number of crescentic glomeruli [17], which represents the severity of complication in GK rats. These data suggest a protective effect of NaHS against oxidative damage. Our data also demonstrated reduced astrogliosis in the NaHS-treated mimetic aging rats in this study (Fig. 2c), suggesting an attenuation of the pathological process that may cause or be closely related with oxidative stress. CD, one of the markers of aging and strongly induced by free radicals, was increased in the D-gal-treated group *in vivo* and *in vitro* (Fig. 7g, h, i), which was in line with previous studies [5,59]. NaHS decreased the occurrence of CD in mitochondria significantly in 3-month-old rats and slightly in 9-month-old rats as well as in cultured neurons (Fig. 7g, h, i). Thus, our data together with other studies demonstrated that NaHS may be beneficial for delaying the process of aging. Abnormal protein homeostasis and mitochondrial dysfunction is also tightly related with the incidence of oxidative stress and aging [1,10]. In our study, NaHS significantly increased the expression of molecular chaperone HSP90 alpha (Fig. 8) and reversed abnormal mitochondria function, as indicated by normalizing the $\Delta\Psi m$ and increasing the ATP production (Fig. 6), with these results being

consistent with a previous study [48]. Therefore, our observations together with other studies may suggest that NaHS plays an advantageous role in postponing aging by increasing antioxidant activity, reducing the incidence of mtDNA mutations, protecting mitochondrial function and improving protein homeostasis, which, ultimately, lower the level of oxidative stress.

4.2. Factors contributing to oxidative stress were inhibited by NaHS through activating CaMKKβ/AMPK and PI3K/AKT pathways

4.2.1. NaHS improved antioxidants via CaMKKβ/AMPK and PI3K/AKT pathways

Organisms and cells are equipped with an antioxidative defense network that balances the generation and ablation of ROS to maintain physical health. Our aging and senescent model manifested reduced activity of the endogenous antioxidant systems such as GSH, SOD and CAT and downregulated expression of antioxidant enzymes such as PRDX2 and TXNRD1, as compared with the controls (Fig. 5). A previous study reported that antioxidant activity declined as aging developed, both in mimetic aging and natural aging rats [34]. It was also reported that NaHS reversed the decreased GSH level and the increased ratio of GSH to oxidized GSH (GSSG) in GK rats, which is characterized by high levels of oxidative stress in the kidney [17]. PRDX2 is sensitive to oxidative stress, especially to low levels of ROS [60]. Similar to PRDX, TXNRD also plays a decisive role in resisting oxidative stress. PRDXs scavenge oxidants such as hydrogen peroxide (H_2O_2) and ROS and, thus, become oxidized and inactive; moreover, TXNRD is critical for the reversion of the inactive PRDX through the use of a hydrogen atom from nicotinamide adenine dinucleotide phosphate (NADPH) [60]. As reported by Padgaonkar and co-workers, TXNRD may play a more important role in protecting cells from stress than GSH [61]. These studies suggested that the antioxidants were consumed gradually during the development of senility. Furthermore, our study demonstrated that NaHS exerts its restorative action on the degraded antioxidant system during aging by enhancing the activity of antioxidants mediated by CaMKKβ/AMPK and PI3K/AKT signaling pathways (Fig. 5a, b, c). In recent studies that aligned with our results, the AMPK and PI3K/AKT pathways were reportedly involved in the regulation of antioxidant activity in oxidative stress models induced by ischemia/reperfusion in mice or H_2O_2 in Leydig's cells [62,63]. In our study, antioxidant enzymes such as PRDX2 and TXNRD1 changed in a similar pattern as the activity of the antioxidants mentioned above *in vivo* and *in vitro* (Fig. 5d). In addition, our data also demonstrated that the expression of PRDX2 and TXNRD1 were decreased during aging but upregulated by NaHS treatment *via* activation of the CaMKKβ/AMPK and PI3K/AKT pathways (Fig. 5d, e). Zha et al. reported that PRDX6 protects cells from oxidative damage *via* PI3K/AKT signaling [64]; this study, together with ours, suggested an intimate relationship between the antioxidant ability and the activation of CaMKKβ/AMPK and PI3K/AKT pathways.

4.2.2. NaHS protected mitochondria via CaMKKβ/AMPK and PI3K/AKT pathways

Oxidative phosphorylation (OXPHOS) is the major process that generates ATP and reactive free radicals. As suggested in our study, the expression of OXPHOS was increased in 3-month-old rats and cultured neurons in D-gal-treated groups, as compared with the controls, particularly complex I and complex II (Fig. 6a, c and Supplementary information Fig. S2). Additionally, ATP production was decreased in the D-gal-treated group, and mitochondrial function, as evaluated by JC-1, was decreased in the group pretreated with D-gal (Fig. 6d). These data suggest that D-gal-induced oxidative stress activates respiration but is accompanied by diminished ATP levels, which have been similarly shown in previous studies [65,66]. Although OXPHOS was activated, an abnormal ΔΨm disturbed ATP production; additionally, while the generation of free radicals increased, apoptosis was consequently augmented. Administration of NaHS downregulated OXPHOS expression and ameliorated the abnormal ΔΨm, eventually protecting mitochondrial function and improving the production of ATP (Fig. 6a, c, d, e and Supplementary information Fig. S2). In the 9-month-old rats, OXPHOS expression was lower than that of the normal control rats (Fig. 6b and Supplementary information Fig. S2). Thus, long-term stress induced by D-gal caused the rats to display more severe aging and rendered the mitochondria dysfunctional, similar to a previous report that the expression of OXPHOS was decreased in aged subjects [67]. The beneficial effects of NaHS on mitochondria were blocked in the groups treated with the inhibitors of PI3K, AMPK and CaMKKβ (Fig. 6c and Supplementary information Fig. S2). A previous study showed that PI3K/AKT activation by overexpression of the first member of Family with sequence similarity 3 gene (FAM3A) protected mitochondrial function, as indicated by increased production of ATP and decreased generation of ROS [68]. In addition, another recent study demonstrated that hepatocellular mitochondria was damaged by hepatotoxic drugs; however, activation of AMPK with AICAR prevented mitochondrial damage, as indicated by reversing abnormal mitochondrial structure, normalizing ΔΨm and increasing ATP production [69]. These studies, together with ours, suggested that the NaHS protection of mitochondrial function is realized through the CaMKKβ/AMPK and PI3K/AKT pathways. Similar with H_2S, nitric oxide (NO), one of another important endogenous gasotransmitter, also involved with the protection of neurons in a proper dose. It preserved the function of mitochondrial biogenesis in neurons and protect neurons from oxidative stress through pathways such as PI3K/AKT [70] and cyclic AMP responsive element binding (CREB) protein [71]. In another words, a potential cross talk exists between the H2S donor and NO in some conditions.

Our data demonstrated that DNA POLG and OGG-1, the mtDNA repair enzymes, were downregulated after D-gal treatment, though they were not noticeably changed in the 3-month-old rats. NaHS significantly improved the expression of DNA POLG and OGG-1 in the mimetic aging rats and senescent cells (Fig. 7a-f). Recently, some studies reported that H_2S was involved in DNA repair of both in nuclear DNA and mtDNA. As reported by Zhao et al., H_2S recruits DNA ligase III to nuclear DNA breaks to mediate the repair of DNA damage, which protects cells from senescence [72]. Another study reported that the mtDNA integrity was protected by a mitochondrially targeted H_2S donor and that mitochondrial activity was preserved [73]. However, these two studies did not report which signaling pathway was involved in the mitochondrial protection mediated by H_2S. These previous results are in parallel with our observation that NaHS increased the mtDNA repair enzymes DNA POLG and OGG-1 and reduced the occurrence of CD (Fig. 7). In addition, as reported by Habib and coworkers, AMPK activation resulted in the upregulation of OGG1 in cancer cells [74]. Thus, on the basis of our observations together with previous studies, a key role of NaHS is suggested for restoring the mtDNA repair ability during aging through activation of the CaMKKβ/AMPK and PI3K/AKT pathways.

4.2.3. NaHS maintains protein homeostasis through CaMKKβ/AMPK and PI3K/AKT pathways

NaHS may also affect proteostasis. In our study, NaHS increased the expression of HSP90 alpha in the mimetic aging rats and senescent cells (Fig. 8a, b, c). Some researchers reported that NaHS protected cells from apoptosis by upregulating HSP90 expression [18]. Conversely, the expression of HSP90 was also stimulated by oxidative stress according to a previous study [75] and our data that showed increased HSP90 in the D-gal-treated group of 3-month-old rats and *in vitro* study (Fig. 8a, c). It may be illustrated that HSP90 alleviates oxidative stress by enhancing the protein folding ability to maintain proteostasis. Meanwhile, our data suggested that CaMKKβ/AMPK and P133K/AKT signaling pathways were involved in the effect of NaHS on regulating HSP90 alpha expression. As previously reported, the effects of NaHS on HSP90 expression depended upon activation of AKT, while a blockade

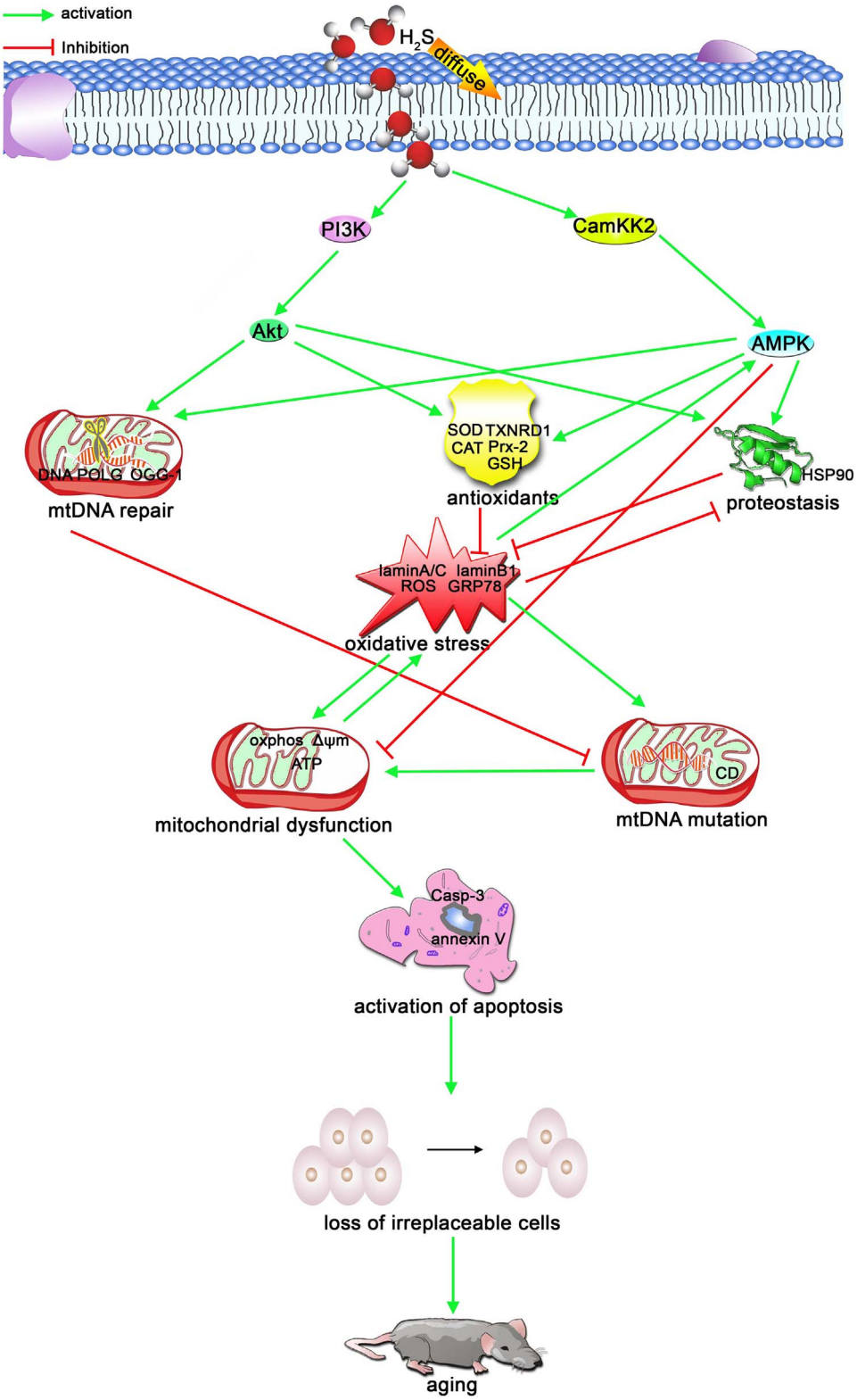

Fig. 9. Schematic illustration of the mechanism for the preventive effect of H_2S on the aging process. Oxidative stress is induced by reduced antioxidants, imbalanced protein homeostasis and dysfunctional mitochondria. Additionally, oxidative stress induces mitochondrial mutations and dysfunction. Mitochondrial mutations are also closely related with the mitochondrial repair function. Mitochondrial dysfunction contributed to the activation of apoptosis and the loss of irreplaceable cells that, ultimately, led to the aging of tissues or organs and age-related disease. Exogenous H_2S attenuates oxidative stress-induced aging by mechanisms that enhance antioxidants, improve mtDNA repair capability and strengthen protein homeostasis (proteostasis). The protective mechanisms were implemented by activation of the PI3K/AKT and CaMKKβ/AMPK pathways.

of AKT significantly decreased the protein abundance of HSP90 *in vitro* [18]. Therefore, integration of these studies demonstrates that CaMKKβ/AMPK and PI3K/AKT were potentially regulatory points for proteostasis initiated by NaHS.

In conclusion, the present observations may identified the beneficial roles of NaHS in protecting neural cells in the auditory cortex against D-gal-induced stress and senility *in vivo* and *in vitro*. CaMKKβ/AMPK and PI3K/AKT probably are two major pathways that are involved in this

protection (Fig. 9). In addition, our data also mirror several important features of aging, which were induced by sustained oxidative stress. Our findings provide some new therapeutic targets for intervening in the aging process and suggest that NaHS may have potential therapeutic value in the treatment of age-related diseases such as presbycusis.

Conflict of interest

None of the authors declare any financial or other conflicts of interest.

Acknowledgments

This work was supported by research grants from National Natural Science Foundations of China (No. 81230021).

Appendix A. Supplementary information

Supplementary data associated with this article can be found in the online version at http://dx.doi.org/10.1016/j.redox.2017.04.031.

References

[1] R.S. Balaban, S. Nemoto, T. Finkel, Mitochondria, oxidants, and aging, Cell 120 (4) (2005) 483–495.
[2] G. Strapazzon, S. Malacrida, A. Vezzoli, T. Dal Cappello, M. Falla, P. Lochner, S. Moretti, E. Procter, H. Brugger, S. Mrakic-Sposta, Oxidative stress response to acute hypobaric hypoxia and its association with indirect measurement of increased intracranial pressure: a field study, Sci. Rep. 6 (2016).
[3] P. Mao, P. Gallagher, S. Nedungadi, M. Manczak, U.P. Shirendeb, S.G. Kohama, B. Ferguson, B.S. Park, P.H. Reddy, Mitochondrial DNA deletions and differential mitochondrial DNA content in Rhesus monkeys: implications for aging, Biochim. Biophys. Acta-Mol. Basis Dis. 1822 (2) (2012) 111–119.
[4] J.A. Nicklas, E.M. Brooks, T.C. Hunter, R. Single, R.F. Branda, Development of a quantitative PCR (TaqMan) assay for relative mitochondrial DNA copy number and the common mitochondrial DNA deletion in the rat, Environ. Mol. Mutagen. 44 (4) (2004) 313–320.
[5] L. Zeng, Y. Yang, Y. Hu, Y. Sun, Z. Du, Z. Xie, T. Zhou, W. Kong, Age-related decrease in the mitochondrial sirtuin deacetylase Sirt3 expression associated with ROS accumulation in the auditory cortex of the mimetic aging rat model, PLos One 9 (2) (2014).
[6] A. Markaryan, E.G. Nelson, R. Hinojosa, Quantification of the Mitochondrial DNA Common Deletion in Presbycusis, Laryngoscope 119 (6) (2009) 1184–1189.
[7] D.C. Wallace, Diseases of the mitochondrial DNA, Annu. Rev. Biochem. 61 (1992) 1175–1212.
[8] S.L. Hebert, I.R. Lanza, K.S. Nair, Mitochondrial DNA alterations and reduced mitochondrial function in aging, Mech. Ageing Dev. 131 (7–8) (2010) 451–462.
[9] S.A. Guaraldo, A.J. Serra, E.M. Amadio, E.L. Antonio, F. Silva, L.A. Portes, P.J. Ferreira Tucci, E.C. Pinto Leal-Junior, Pd.T. Camillo de Carvalho, The effect of low-level laser therapy on oxidative stress and functional fitness in aged rats subjected to swimming: an aerobic exercise, Lasers Med. Sci. 31 (5) (2016) 833–840.
[10] J. Labbadia, R.I. Morimoto, The biology of proteostasis in aging and disease (84), Annu. Rev. Biochem. 84 (2015) 435–464.
[11] R.A. Floyd, K. Hensley, Oxidative stress in brain aging - implications for therapeutics of neurodegenerative diseases, Neurobiol. Aging 23 (5) (2002) 795–807.
[12] J. Sun, H. Wang, B. Liu, W. Shi, J. Shi, Z. Zhang, J. Xing, Rutin attenuates H2O2-induced oxidation damage and apoptosis in Leydig cells by activating PI3K/Akt signal pathways, Biomed. Pharmacother. 88 (2017) 500–506.
[13] C.-Y. Tsai, C.-C. Wang, T.-Y. Lai, H.-N. Tsu, C.-H. Wang, H.-Y. Liang, W.-W. Kuo, Antioxidant effects of diallyl trisulfide on high glucose-induced apoptosis are mediated by the PI3K/Akt-dependent activation of Nrf2 in cardiomyocytes, Int. J. Cardiol. 168 (2) (2013) 1286–1297.
[14] U. Shefa, S.G. Yeo, M.-S. Kim, I.O. Song, J. Jung, N.Y. Jeong, Y. Huh, Role of Gasotransmitters in Oxidative Stresses, Neuroinflammation, and Neuronal Repair, BioMed. Res. Int. 2017 (2017) (1689341-1689341).
[15] N. Sen, Functional and Molecular Insights of Hydrogen Sulfide Signaling and Protein Sulfhydration, J. Mol. Biol.
[16] Y.H. Chen, W.Z. Yao, B. Geng, Y.L. Ding, M. Lu, M.W. Zhao, C.S. Tang, Endogenous hydrogen sulfide in patients with COPD, Chest 128 (5) (2005) 3205–3211.
[17] R. Xue, D.-D. Hao, J.-P. Sun, W.-W. Li, M.-M. Zhao, X.-H. Li, Y. Chen, J.-H. Zhu, Y.-J. Ding, J. Liu, Y.-C. Zhu, Hydrogen Sulfide Treatment Promotes Glucose Uptake by Increasing Insulin Receptor Sensitivity and Ameliorates Kidney Lesions in Type 2 Diabetes, Antioxid. Redox Signal. 19 (1) (2013) 5–23.
[18] L. Xie, C.X. Tiong, J.-S. Bian, Hydrogen sulfide protects SH-SY5Y cells against 6-hydroxydopamine-induced endoplasmic reticulum stress, Am. J. Physiol.-Cell Physiol. 303 (1) (2012) C81–C91.
[19] P.K. Kamat, A. Kalani, S.C. Tyagi, N. Tyagi, Hydrogen sulfide epigenetically attenuates homocysteine-induced mitochondrial toxicity mediated through NMDA receptor in mouse brain endothelial (bEnd3) cells, J. Cell. Physiol. 230 (2) (2015) 378–394.
[20] P. Cheng, F. Wang, K. Chen, M. Shen, W. Dai, L. Xu, Y. Zhang, C. Wang, J. Li, J. Yang, R. Zhu, H. Zhang, Y. Zheng, J. Lu, Y. Zhou, C. Guo, Hydrogen sulfide ameliorates ischemia/reperfusion-induced hepatitis by inhibiting apoptosis and autophagy pathways, Mediat. Inflamm. (2014).
[21] A. Melendez, Z. Talloczy, M. Seaman, E.L. Eskelinen, D.H. Hall, B. Levine, Autophagy genes are essential for dauer development and life-span extension in C-elegans, Science 301 (5638) (2003) 1387–1391.
[22] X. Yu, Y.C. Long, H.-M. Shen, Differential regulatory functions of three classes of phosphatidylinositol and phosphoinositide 3-kinases in autophagy, Autophagy 11 (10) (2015) 1711–1728.
[23] D. Tang, Q.-B. Chen, X.-L. Xin, H.-A. Aisa, Anti-diabetic effect of three new norditerpenoid alkaloids in vitro and potential mechanism via PI3K/Akt signaling pathway, Biomed. Pharmacother. 87 (2017) 145–152.
[24] G. Ambrosini, E. Musi, A.L. Ho, E. de Stanchina, G.K. Schwartz, Inhibition of mutant GNAQ signaling in uveal melanoma induces AMPK-dependent autophagic cell death, Mol. Cancer Ther. 12 (5) (2013) 768–776.
[25] A. Salminen, A. Kauppinen, K. Kaarniranta, FGF21 activates AMPK signaling: impact on metabolic regulation and the aging process, J. Mol. Med. 95 (2) (2017) 123–131.
[26] G.A. Gates, J.H. Mills, Presbycusis, Lancet 366 (9491) (2005) 1111–1120.
[27] X. Cui, P. Zuo, Q. Zhang, X. Li, Y. Hu, J. Long, L. Packer, J. Liu, Chronic systemic D-galactose exposure induces memory loss, neuro degeneration, and oxidative damage in mice: protective effects of R-alpha-lipoic acid, J. Neurosci. Res. 84 (3) (2006) 647–654.
[28] J.Y. Woo, W. Gu, K.A. Kim, S.E. Jang, M.J. Han, D.H. Kim, Lactobacillus pentosus var. plantarum C29 ameliorates memory impairment and inflammaging in a D-galactose-induced accelerated aging mouse model, Anaerobe 27 (2014) 22–26.
[29] L.L. Zeng, Y. Yang, Y.J. Hu, Y. Sun, Z.D. Du, Z. Xie, T. Zhou, W.J. Kong, Age-related decrease in the mitochondrial sirtuin deacetylase Sirt3 expression associated with ROS accumulation in the auditory cortex of the mimetic aging rat model, Plos One 9 (2) (2014).
[30] B. Chen, Y. Zhong, W. Peng, Y. Sun, W.-J. Kong, Age-related changes in the central auditory system: comparison of D-galactose-induced aging rats and naturally aging rats, Brain Res. 1344 (2010) 43–53.
[31] B. Chen, Y. Zhong, W. Peng, Y. Sun, W.J. Kong, Age-related changes in the central auditory system: comparison of D-galactose-induced aging rats and naturally aging rats, Brain Res. 1344 (2010) 43–53.
[32] C. Wang, J.A. Kaufmann, M.G. Sanchez-Ross, K.M. Johnson, Mechanisms of N-methyl-D-aspartate-induced apoptosis in phencyclidine-treated cultured forebrain neurons, J. Pharmacol. Exp. Ther. 294 (1) (2000) 287–295.
[33] X. Chen, X. Zhao, Y. Hu, F. Lan, H. Sun, G. Fan, Y. Sun, J. Wu, W. Kong, The spread of adenoviral vectors to central nervous system through pathway of cochlea in mimetic aging and young rats, Gene Ther. 22 (11) (2015) 866–875.
[34] H.-Y. Sun, Y.-J. Hu, X.-Y. Zhao, Y. Zhong, L.-L. Zeng, X.-B. Chen, J. Yuan, J. Wu, Y. Sun, W. Kong, W.-J. Kong, Age-related changes in mitochondrial antioxidant enzyme Trx2 and TXNIP-Trx2-ASK1 signal pathways in the auditory cortex of a mimetic aging rat model: changes to Trx2 in the auditory cortex, Febs J. 282 (14) (2015) 2758–2774.
[35] N.J. Forcier, A.P. Mizisin, M.A. Rimmer, H.C. Powell, Cellular pathology of the nerve microenvironment in galactose intoxication, J. Neuropathol. Exp. Neurol. 50 (3) (1991) 235–255.
[36] I.J. Lee, C.-W. Lee, J.-H. Lee, CaMKK beta-AMPK alpha 2 signaling contributes to mitotic Golgi fragmentation and the G2/M transition in mammalian cells, Cell Cycle 14 (4) (2015) 598–611.
[37] K.A. Anderson, T.J. Ribar, F. Lin, P.K. Noeldner, M.F. Green, M.J. Muehlbauer, L.A. Witters, B.E. Kemp, A.R. Means, Hypothalamic CaMKK2 contributes to the regulation of energy balance, Cell Metab. 7 (5) (2008) 377–388.
[38] D. Morales-Alamo, J.A.L. Calbet, AMPK signaling in skeletal muscle during exercise: role of reactive oxygen and nitrogen species, Free Radic. Biol. Med. 98 (2016) 68–77.
[39] J.A. McCubrey, D. Rakus, A. Gizak, L.S. Steelman, S.L. Abrams, K. Lertpiriyapong, T.L. Fitzgerald, L.V. Yang, G. Montalto, M. Cervello, M. Libra, F. Nicoletti, A. Scalisi, F. Torino, C. Fenga, L.M. Neri, S. Marmiroli, L. Cocco, A.M. Martelli, Effects of mutations in Wnt/beta-catenin, hedgehog, Notch and PI3K pathways on GSK-3 activity-Diverse effects on cell growth, metabolism and cancer, Biochim. Biophys. Acta-Mol. Cell Res. 1863 (12) (2016) 2942–2976.
[40] L. Racioppi, A.R. Means, Calcium/calmodulin-dependent protein kinase kinase 2: roles in signaling and pathophysiology, J. Biol. Chem. 287 (38) (2012) 31658–31665.
[41] G.S. Hotamisligil, Endoplasmic reticulum stress and atherosclerosis, Nat. Med. 16 (4) (2010) 396–399.
[42] T. Dechat, S.A. Adam, P. Taimen, T. Shimi, R.D. Goldman, Nuclear lamins, Cold Spring Harb. Perspect. Biol. 2 (11) (2010).
[43] A. Barascu, C. Le Chalony, G. Pennarun, D. Genet, N. Imam, B. Lopez, P. Bertrand, Oxidative stress induces an ATM-independent senescence pathway through p38 MAPK-mediated lamin B1 accumulation, EMBO J. 31 (5) (2012) 1080–1094.
[44] M. Pekny, M. Pekna, Astrocyte reactivity and reactive astrogliosis: costs and benefits, Physiol. Rev. 94 (4) (2014) 1077–1098.
[45] D. Coling, S. Chen, L.-H. Chi, S. Jamesdaniel, D. Henderson, Age-related changes in antioxidant enzymes related to hydrogen peroxide metabolism in rat inner ear, Neurosci. Lett. 464 (1) (2009) 22–25.
[46] F. Hattori, S. Oikawa, Peroxiredoxins in the central nervous system, Subcellular, Biochemistry 44 (2007) 357–374.

[47] E.S.J. Arner, Focus on mammalian thioredoxin reductases - Important selenoproteins with versatile functions, Biochim. Biophys. Acta-General. Subj. 1790 (6) (2009) 495–526.
[48] C. Szabo, C. Ransy, K. Modis, M. Andriamihaja, B. Murghes, C. Coletta, G. Olah, K. Yanagi, F. Bouillaud, Regulation of mitochondrial bioenergetic function by hydrogen sulfide. Part I. Biochemical and physiological mechanisms, Br. J. Pharmacol. 171 (8) (2014) 2099–2122.
[49] F.M. Yakes, B. VanHouten, Mitochondrial DNA damage is more extensive and persists longer than nuclear DNA damage in human cells following oxidative stress, Proc. Natl. Acad. Sci. USA 94 (2) (1997) 514–519.
[50] P. Boesch, F. Weber-Lotfi, N. Ibrahim, V. Tarasenko, A. Cosset, F. Paulus, R.N. Lightowlers, A. Dietrich, DNA repair in organelles: pathways, organization, regulation, relevance in disease and aging, Biochim. Et. Biophys. Acta-Mol. Cell Res. 1813 (1) (2011) 186–200.
[51] Y. Nakabeppu, Regulation of intracellular localization of human MTH1, OGG1, and MYH proteins for repair of oxidative DNA damage (68), Progress. Nucleic Acid. Res. Mol. Biol. 68 (2001) 75–94.
[52] M.A. Graziewicz, M.J. Longley, W.C. Copeland, DNA polymerase gamma in mitochondrial DNA replication and repair, Chem. Rev. 106 (2) (2006) 383–405.
[53] W.J. Kong, Y.J. Hu, Q.O. Wang, Y. Wang, Y.C. Han, H.M. Cheng, W. Kong, M.X. Guan, The effect of the mtDNA4834 deletion on hearing, Biochem. Biophys. Res. Commun. 344 (1) (2006) 425–430.
[54] N. Kaneko, A. Vierkoetter, U. Kraemer, D. Sugiri, M. Matsui, A. Yamamoto, J. Krutmann, A. Morita, Mitochondrial common deletion mutation and extrinsic skin ageing in German and Japanese women, Exp. Dermatol. 21 (2012) 26–30.
[55] H. Koga, S. Kaushik, A.M. Cuervo, Protein homeostasis and aging: the importance of exquisite quality control, Ageing Res. Rev. 10 (2) (2011) 205–215.
[56] M. Taipale, I. Krykbaeva, M. Koeva, C. Kayatekin, K.D. Westover, G.I. Karras, S. Lindquist, Quantitative analysis of Hsp90-client interactions reveals principles of substrate recognition, Cell 150 (5) (2012) 987–1001.
[57] B. Chen, W.H. Piel, L.M. Gui, E. Bruford, A. Monteiro, The HSP90 family of genes in the human genome: insights into their divergence and evolution, Genomics 86 (6) (2005) 627–637.
[58] M.P. Gavilan, J. Vela, A. Castano, B. Ramos, J.C. del Rio, J. Vitorica, D. Ruano, Cellular environment facilitates protein accumulation in aged rat hippocampus, Neurobiol. Aging 27 (7) (2006) 973–982.
[59] X.Y. Zhao, J.L. Sun, Y.J. Hu, Y. Yang, W.J. Zhang, Y. Hu, J. Li, Y. Sun, Y. Zhong, W. Peng, H.L. Zhang, W.J. Kong, The effect of overexpression of PGC-1 alpha on the mtDNA4834 common deletion in a rat cochlear marginal cell senescence model, Hear. Res. 296 (2013) 13–24.
[60] M.H. Park, M. Jo, Y.R. Kim, C.-K. Lee, J.T. Hong, Roles of peroxiredoxins in cancer, neurodegenerative diseases and inflammatory diseases, Pharmacol. Ther. 163 (2016) 1–23.
[61] V.A. Padgaonkar, V.R. Leverenz, A.V. Bhat, S.E. Pelliccia, F.J. Giblin, Thioredoxin reductase activity may be more important than GSH level in protecting human lens epithelial cells against UVA light, Photochem. Photobiol. 91 (2) (2015) 387–396.
[62] J. Duan, Y. Guan, F. Mu, C. Guo, E. Zhang, Y. Yin, G. Wei, Y. Zhu, J. Cui, J. Cao, Y. Weng, Y. Wang, M. Xi, A. Wen, Protective effect of butin against ischemia/reperfusion-induced myocardial injury in diabetic mice: involvement of the AMPK/GSK-3 beta/Nrf2 signaling pathway beta/Nrf2 signaling pathway, Sci. Rep. 7 (2017).
[63] J. Sun, H. Wang, B. Liu, W. Shi, J. Shi, Z. Zhang, J. Xing, Rutin attenuates H2O2-induced oxidation damage and apoptosis in Leydig cells by activating PI3K/Azkt signal pathways, Biomed. Pharmacother. = Biomed. Pharmacother. 88 (2017) 500–506.
[64] X. Zha, G. Wu, X. Zhao, L. Zhou, H. Zhang, J. Li, L. Ma, Y. Zhang, PRDX6 protects ARPE-19 cells from oxidative damage via PI3K/AKT signaling, Cell. Physiol. Biochem. 36 (6) (2015) 2217–2228.
[65] N. Yadav, A. Pliss, A. Kuzmin, P. Rapali, L. Sun, P. Prasad, D. Chandra, Transformations of the macromolecular landscape at mitochondria during DNA-damage-induced apoptotic cell death, Cell Death Dis. 5 (2014).
[66] B. He, H. Guo, Y. Gong, R. Zhao, Lipopolysaccharide-induced mitochondrial dysfunction in boar sperm is mediated by activation of oxidative phosphorylation, Theriogenology 87 (2017) 1–8.
[67] H. Bakala, R. Ladouce, M.A. Baraibar, B. Friguet, Differential expression and glycative damage affect specific mitochondrial proteins with aging in rat liver, Biochim. Biophys. Acta-Mol. Basis Dis. 1832 (12) (2013) 2057–2067.
[68] Q. Song, W.-L. Gou, R. Zhang, FAM3A Protects HT22 Cells Against Hydrogen Peroxide-Induced Oxidative Stress Through Activation of PI3K/Akt but not MEK/ERK Pathway, Cell. Physiol. Biochem. 37 (4) (2015) 1431–1441.
[69] S.W.S. Kang, G. Haydar, C. Taniane, G. Farrell, I.M. Arias, J. Lippincott-Schwartz, D. Fu, AMPK activation prevents and reverses drug-induced mitochondrial and hepatocyte injury by promoting mitochondrial fusion and function, PLoS One 11 (10) (2016).
[70] A. Contestabile, E. Ciani, Role of nitric oxide in the regulation of neuronal proliferation, survival and differentiation, Neurochem. Int. 45 (6) (2004) 903–914.
[71] A. Riccio, R.S. Alvania, B.E. Lonze, N. Ramanan, T. Kim, Y.F. Huang, T.M. Dawson, S.H. Snyder, D.D. Ginty, A nitric oxide signaling pathway controls CREB-mediated gene expression in neurons, Mol. Cell 21 (2) (2006) 283–294.
[72] K. Zhao, Y. Ju, S. Li, Z. Altaany, R. Wang, G. Yang, S-sulfhydration of MEK1 leads to PARP-1 activation and DNA damage repair, EMBO Rep. 15 (7) (2014) 792–800.
[73] B. Szczesny, K. Modis, K. Yanagi, C. Coletta, S. Le Trionnaire, A. Perry, M.E. Wood, M. Whiteman, C. Szabo, AP39, a novel mitochondria-targeted hydrogen sulfide donor, stimulates cellular bioenergetics, exerts cytoprotective effects and protects against the loss of mitochondrial DNA integrity in oxidatively stressed endothelial cells in vitro, Nitric Oxide-Biol. Chem. 41 (2014) 120–130.
[74] S.L. Habib, B.S. Kasinath, R.R. Arya, S. Vexler, C. Velagapudi, Novel mechanism of reducing tumourigenesis: upregulation of the DNA repair enzyme OGG1 by rapamycin-mediated AMPK activation and mTOR inhibition, Eur. J. Cancer 46 (15) (2010) 2806–2820.
[75] M. Chen, P.Y. Sato, J.K. Chuprun, R.J. Peroutka, N.J. Otis, J. Ibetti, S. Pan, S.-S. Sheu, E. Gao, W.J. Koch, Prodeath Signaling of G protein-coupled receptor kinase 2 in cardiac myocytes after ischemic stress occurs via extracellular signal-regulated kinase-dependent heat shock protein 90-mediated mitochondrial Targeting, Circ. Res. 112 (8) (2013) (1121-+).